Effects along the epithelial-mesenchymal biointerface in direct cell self-organisation: multiscale theoretical analysis

Ivana Pajic-Lijakovic [1], Milan Milivojevic [1], and Peter V. E. McClintock[2]

[1] University of Belgrade, Faculty of Technology and Metallurgy, Department of Chemical Engineering, Belgrade, Serbia

[2] Department of Physics, Lancaster University, Lancaster LA1 4YB, UK

Correspondence to: Ivana Pajic-Lijakovic, iva@tmf.bg.ac.rs

Peter V. E. McClintock, p.v.e.mcclintock@lancaster.ac.uk

Abstract

Epithelial cancer ranks among the most deadly types of cancer globally. Focusing on the disease's early stages could lead to significant enhancements in the survival rates of cancer patients. The initial phase of the disease is associated with the dissemination of cancer cells into the adjacent healthy epithelium. Therefore, a more profound understanding of cell dynamics at the biointerface between epithelial and cancer (mesenchymal) cells is essential for managing the disease promptly. The dynamics of cells at this epithelial-cancer biointerface arises through interplay between a variety of biological and physical mechanisms. Although considerable research has been dedicated to examining the spread of cancer cells across the epithelium, the physical mechanisms that govern the dynamics at the biointerface remain poorly understood. The main goal of this multi-scale theoretical consideration is to emphasize the influence of physical factors, such as the viscoelasticity of the subpopulations and the dilational viscoelasticity of the biointerface, on the efficiency with which cancer spreads through the epithelium. We do so by consideration of the mechanical coupling between the epithelial and cancer mesenchymal-like subpopulations. In this review, we consider this complex phenomenon from a multiscale mechanical perspective that has not been explicitly addressed in earlier studies, using model systems such as the segregation of co-cultured epithelial–mesenchymal spheroids. The mechanical-coupling between the subpopulations arising from the system's viscoelasticity is discussed from the cellular to supracellular levels in order to recognize the main physical factors responsible for the spreading of cancer.

Key words: collective cell migration; efficiency of segregation; viscoelasticity;, multi-scale mathematical modeling; heterotypic cell-cell interactions

Glossary of terms

Epithelial cells: exhibit cuboidal shape, limited mobility, apical-basal polarity, and strong E-cadherin-mediated cell-cell adhesions

Epithelial-to-mesenchymal transition:**(EMT):** a biological process in which epithelial cells partially or fully lose epithelial characteristics and acquire mesenchymal-like properties, leading to profound changes in adhesion, mechanics, and motility.

Mesenchymal cells: exhibit an elongated shape, increased migratory ability, front-rear cell polarity, and weak N-cadherin-mediated cell-cell adhesion.

Segregation: self-organization of epithelial and mesenchymal subpopulations within co-cultured spheroids such that epithelial cells migrate towards the spheroid core region, while cancer cells migrate towards the spheroid surface region.

Spheroids: cell aggregates of size an order of magnitude or larger than the size of a single cell.

Viscoelasticity: a property of material, which defines the elastic and viscous characteristics of the system when it undergoes deformation.

1.Introduction

Comprehending the mechanisms that regulate tumor invasion is essential both for fundamental cancer research and for its clinical applications. Earlier *in vivo* investigations have indicated that invasive epithelial cancer cells separate from the primary tumor and, in the form of mesenchymal-like cancer cells infiltrate the surrounding healthy epithelial tissue, leading to an irregular invasive morphology (Millar et al., 2017; Campbell et al., 2019; Riehl et al., 2021). Although the movements of cells associated with tumor invasion are driven by the mechanical forces of epithelial-mesenchymal interactions, the manner in which these mechanical properties influence tumor invasion is still not well understood. Mechanical coupling refers to how these two distinct cell types interact physically and influence each other's mechanical and rheological behaviour, either at their biointerface or within a mixed tissue (Friedl and Gilmour, 2009). Kachalo et al. (2015) and Li et al. (2014) indicated that the tension between cells and the pressure within cells were the main physical factors contributing to cell rearrangement via collective cell migration. The impact of these parameters on cell response was discussed in terms of the Pott model, formulated on the cellular level (Kachalo et al., 2015; Li et al., 2014).

Li et al. (2014) pointed out that invasive cancer mesenchymal-like cells should exhibit (i) increased adhesion to the extracellular matrix (ECM) and (ii) decreased cell-cell adhesion. The efficiency of cell migration has been connected with the viscoelasticity of multicellular systems (Pajic-Lijakovic, et al., 2024a). To gain a comprehensive understanding of the physical mechanisms governing tumor invasion, we will examine the influence of dynamics within epithelial and mesenchymal subpopulations (**Glossary of terms**) that are in direct contact. The phenomenon will be discussed on a simple model system in

which the segregation of these subpopulations occurs through collective cell migration within co-cultured spheroids. Cell migration is an intrinsically active, non-equilibrium process that requires continuous metabolic energy input, primarily in the form of ATP. Actin-driven migration is powered by actin polymerization and myosin motor activity (Pollard and Borisy, 2003) which generate protrusive and contractile forces, while water-driven migration relies on ATP-dependent ion pumps that maintain osmotic gradients driving directed fluid fluxes (Stroka et al., 2014). In both cases, the energy is not stored as elastic or interfacial energy but is continuously dissipated through cytoskeletal remodeling, adhesion turnover, and viscous losses.

Although individual cell migration exists, the focus here is placed on collective migration because both epithelial tissues and co-cultured epithelial–cancer spheroids reorganize predominantly through coordinated, collective migration (Kabla, 2012). Collective cell migration results in local extension, compression and shear of multicellular systems leading to the generation of mechanical stress (Serra-Picamal et al., 2012; Notbohm et al., 2016; Pajic-Lijakovic et al., 2024b). Changes in cell organization lead to energy storage and dissipation, which are characteristic features of viscoelasticity, in multicellular systems (Pajic-Lijakovic et al., 2025a). Energy dissipation arises as a consequence of the remodelling of cell-cell and cell-matrix adhesion contacts and perturbation of cell alignment, causing contact inhibition of locomotion (Pajic-Lijakovic and Milivojevic, 2025a). While the remodelling of adhesion contacts occurs over minutes, cell repolarisation takes place over hours, indicating various mechanisms of energy dissipation (Lee and Wolgemuth, 2011; Notbohm et al., 2016; Pajic-Lijakovic et al., 2025a). Energy dissipation caused by the remodeling of cell-cell adhesion contacts facilitates the relaxation of mechanical stress within the epithelial and mesenchymal subpopulations (Marmottant et al., 2009; Pajic-Lijakovic et al., 2023a). Stress relaxation in this way depends on the cell packing density and has been confirmed experimentally to occur for densities lower than or equal to the cell packing density in the confluent state (Pajic-Lijakovic and Milivojevic, 2021). Higher cell packing density can suppress stress relaxation.

While mesenchymal cells shield themselves effectively from the influence of increased cell packing density in bulk regions, this is not true of epithelial collectives for which increased density can lead to the epithelial cell jamming state (i.e., a shift from contractile to non-contractile behavior) (Grosser et al., 2021; Tlili et al., 2018). Consequently, the migration of mesenchymal cells is more efficient than that of epithelial cells. The differing behaviours exhibited by these cell populations are largely attributed to the varying strengths of their cell-cell adhesion contacts (Barriga and Mayor, 2019; Pajic-Lijakovic and Milivojevic, 2021). Epithelial cells form strong E-cadherin-mediated adhesion contacts, whereas mesenchymal cells develop weaker N-cadherin-mediated adhesion contacts (Barriga and Mayor, 2019). These weaker cell-cell adhesion contacts serve to protect mesenchymal cells from excessive energy storage and the generation of compressive stress. This aligns with the understanding that energy storage occurs within adhesion junctions and the cytoskeleton.

The interplay between the viscoelastic properties of the subpopulations and the heterotypic interactions at the biointerface is analyzed theoretically by emphasizing the impact of these interactions on mechanical coupling between the subpopulations. The formation and maintenance of accurately arranged tissues depend on sharp biointerfaces between diverse cell populations, as noted by Batlle and

Wilkinson (2012). However, the epithelial-to-mesenchymal transition along the biointerface can lead to the formation of a perturbed and diffusive biointerface. This multi scale modeling approach seeks to: highlight the impact of mechanical coupling between the subpopulations on the spreading of cancer and (ii) encourage additional experiments in the area, despite the fact that calculations derived from this model set are currently unfeasible for the reasons had we now discuss.

Current experimental evidence about complex dynamics along the biointerface between epithelial and mesenchymal subpopulations is limited. Morphological changes of epithelial and mesenchymal subpopulations within co-cultured spheroids have been monitored, but without direct measurement of important physical parameters (Carey et al., 2013; Devanny et al., 2021). Physical parameters such as cell packing density, mechanical stress, and the strain caused by collective cell migration have been measured in cell monolayers rather than in cell spheroids (Serra-Picamal et al., 2012; Nnetu et al., 2013, Notbohm et al., 2016; Tlili et al., 2018). Tissue surface tension has been measured under simplified conditions by micropipette aspiration (Guevorkian et al., 2021) and cell aggregate uniaxial compression between parallel plates (Marmottant et al., 2009). These techniques offer the ability to measure an equilibrium value of the epithelial surface tension (i.e., a static surface tension). Nevertheless, tissue surface tension is a physical parameter that varies with space and time. The interfacial tension between epithelial and mesenchymal cells is influenced by the surface tensions of the subpopulations as well as by the interaction potential between them, which has yet to be measured.

In previous papers, we pointed to the importance of the epithelial mesenchymal interfacial tension in the dynamics along the biointerface (Pajic-Lijakovic et al., 2025b) and the generation of flow-instabilities caused by shear stress along the biointerface (Pajic-Lijakovic et al., 2023b). The main focus of our present theoretical consideration is to discuss the mechanical coupling between the subpopulations, spanning from the cellular to the supracellular levels, a range that affects the efficacy of the segregation process and the spreading of cancer.

2. Morphology of epithelial subpopulation in co-cultured epithelial-mesenchymal spheroids and the biointerface size

Epithelial and mesenchymal subpopulations migrate collectively within co-cultured spheroids during the segregation process in order to minimise the free energy of rearrangement and the area of the biointerface. The segregation process depends primarily on the difference between the surface tensions of the subpopulations (Méhes et al., 2023). Given that the epithelial subpopulation is more cohesive than the mesenchymal subpopulation, it may be regarded as a dispersed pseudo-phase, whereas the mesenchymal subpopulation is characterized as a continuum phase. The size of the biointerface depends on the size of epithelial clusters if the number of epithelial cells is approximately constant. Cell division, which may contribute to an increase in cell numbers, can be disregarded on a time frame of hours, as it typically transpires over a significantly longer duration (days) for many cell types, including those examined in this study, which include epithelial MCF-10A cells, human keratinocytes, MDCK cells,

and breast mesenchymal MDA-MB-231 cells (Pajic-Lijakovic et al., 2024b). Furthermore, the doubling time of epithelial cells is extended under conditions of overcrowding.

The epithelial subpopulation undergoes collective cell migration toward the core regions of spheroids, driven by epithelial surface tension, while the mesenchymal subpopulation migrates towards the spheroid surface driven by mechanical stress accumulated in the core region (Carey et al., 2013; Devanny et al., 2021; Pajic-Lijakovic et al., 2024a). Whether epithelial cells undergo complete or partial segregation depends on the difference between their cohesion. Various morphologies of epithelial cells in contact with cancer cells are shown in **Figure 1**:

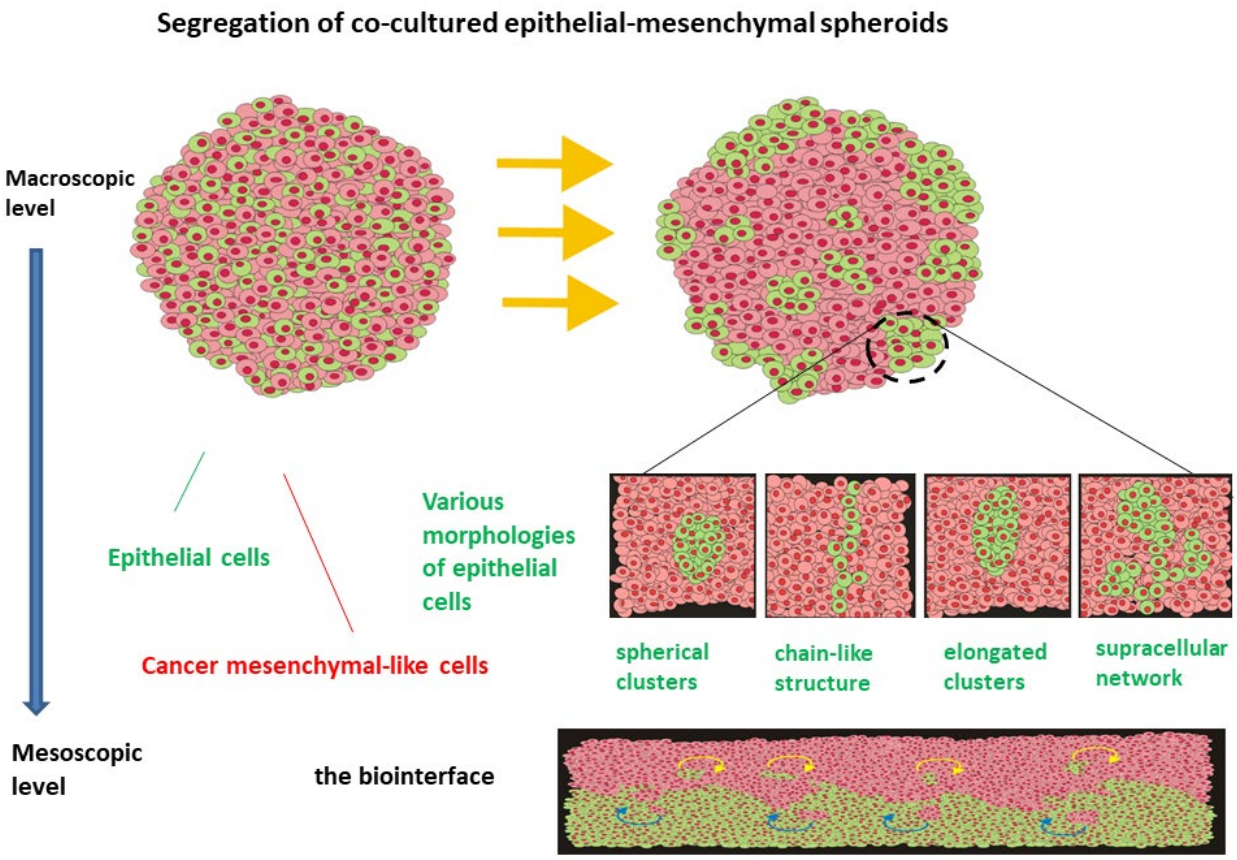

Figure 1. Various morphologies of epithelial cells in contact with cancer cells within co-cultured spheroids influence the size of the biointerface area and, on that basis, the mechanical coupling between the subpopulations. While epithelial cells migrate toward the spheroid core, mesenchymal cells migrate toward its surface. Yellow and blue arrows show the directions of their migration along the biointerface. Circular movement of the subpopulations is caused by shear stress (Pajic-Lijakovic and Milivojevic, 2023b). Perturbation of the biointerface is induced by the interplay between mechanical stress and the epithelial-to-mesenchymal transition. Epithelial cells, as a dispersed subpopulation, can form various morphologies depending on the interfacial tension and friction effects along the biointerface (Pajic-Lijakovic and Milivojevic, 2023c). While the interfacial tension tends to minimise the

interfacial area and form smaller-sized, spherical clusters, frictional effects can cause elongation of these clusters. Collision between epithelial clusters can induce the formation of a supracellular network-like structure. All of these morphologies have an impact on the size of the biointerface.

The properties and mechanism of segregation of various co-cultured multicellular systems are presented in **Table 1**:

Table 1. The properties and mechanism of segregation of various co-cultured multicellular systems

epithelial-cancer multicellular systems*	Segregation	Mechanism	Reference
Spheroids: MCF10A-MDA-MB-231	 Complete	cancer cells act as leader cells at the front of a multicellular cohort, mechanically guiding the collective movement	Carey et al. (2013)
Spheroids: MCF10A-MDA-MB-231 MCF10A-MDA-MB-468 MCF10A-MDA-MB-436 MCF10A-MDA-MB-157 MDA-MB-468- MDA-MB-157	 Complete Partial Complete Complete Partial	The mismatch in surface tension between epithelial and cancer cells creates an effective mechanical barrier at the interface	Devanny et al. (2021)
Monolayers: MDCK II- C2C12 HaCaT- C2C12	 Partial Partial	collision-mediated mechanical interactions at the biointerface induce the generation of mechanical stress	Lucia et al., 2022
Monolayers: MCF10A-MDA-MB-231	 Complete	mechanical coupling and biochemical signaling between subpopulations	Heine et al. (2021)
Monolayers: HaCaT - HT1080	 Partial	heterotypic contact inhibition of locomotion (CIL). The segregation depends on EphB2 and ERK signaling.	Brayford et al. (2019)

*Consisting of Madin-Darby canine kidney type II (MDCK II) epithelial cells, keratinocytes (HaCaT), mouse myoblast mesenchymal (C2C12) cells, breast epithelial cells (MCF10A), breast cancer mesenchymal-like cell types (MDA-MB-231, MDA-MB-468, MDA-MB-436, MDA-MB-157), and fibroblasts (NIH3T3).

The breast epithelial MCF-10A cells develop compact spheroids in mono-cultured systems. In contrast, within co-cultured cellular systems, these cells exhibit either partial or complete segregation, influenced by the cohesion of the cancer subpopulation and heterotypic cell-cell interactions along the biointerface. Co-cultured systems are established through a two-step process. Initially, epithelial and mesenchymal subpopulations are cultured independently before being mixed (Huang et al., 2020). In the co-cultured systems of MDA-MB-436/MCF-10A and MDA-MB-231/MCF-10A, complete segregation occurs. In these examples, more cohesive MCF-10A cells, characterized by higher surface tension, extend towards the core region of the spheroid, while the MDA-MB-231 (or MDA-MB-436) cells, which possess significantly lower tissue surface tension, occupy the surface region of the spheroid (Carey et al., 2013; Devanny et al., 2021). Conversely, in co-culture with MDA-MB-468 cells, the MCF-10A cells demonstrate partial segregation (Devanny et al., 2021). ZR-75-1 cells possess the ability to express both β_1 integrin and E-cadherin, resulting in a higher surface tension when compared to MDA-MB-468 cells

(Devanny et al., 2021). The co-cultured cellular systems of MDA-MB-468 and MDA-MB-157 exhibit partial segregation. This observation aligns with the fact that MDA-MB-157 cells do not express E-cadherin; however, they can form cell-cell adhesion contacts through alternative cadherin types, thereby achieving increased surface tension (Devanny et al., 2021). Additionally, MDA-MB-468 cells are capable of forming mixed spheroids in conjunction with MDA-MB-436 cells (Devanny et al., 2021).

Note that, while *in vitro* spheroid co-culture systems capture many aspects of multicellular organization and collective migration, they remain simplified models that lack essential features of the *in vivo* tumor microenvironment, such as functional blood vessels, immune cell populations, complete extracellular matrix (ECM) architecture, and physiological gradients of oxygen and nutrients. These missing components profoundly influence tissue rheology, interstitial fluid pressures, and mechanotransduction pathways, all of which modulate cell mechanics, migration, and segregation behaviour in actual tumors (Mierke, 2024).

3. Modelling of the segregation process

Segregation during collective cell migration has been modelled using Potts, vertex, and phase-field approaches. The Potts model uses a lattice-based stochastic framework to minimize an effective energy that accounts for interfacial tension and cell area constraints (Graner and Glazier, 2016), allowing detailed investigation of cell-scale rearrangements, though shape fluctuations depend on an abstract temperature parameter (Alert and Trepat, 2020). Phase-field models describe cells as continuous fields, encoding interactions in a free energy functional and treating migrating collectives as viscous polar liquids and describe cell shape via a contour function (Coburn et al., 2013). Vertex models describe epithelial tissues as networks of polygonal cells, focusing on junctional tension, cell shape (area and perimeter), and topological rearrangements such as neighbour exchange (Fletcher et al., 2014; Alt et al., 2017). Common characteristics of these cellular-scale models are that they do not include the viscoelasticity of multicellular systems, which is crucial for understanding collective cell migration and the segregation process. Viscoelastic properties depend on cell packing density, which in turn feeds back on the physical mechanisms of cell migration and tissue cohesion. Capturing this cause–effect relationship requires a supracellular modeling framework. Our framework complements these approaches by introducing explicit surface viscoelasticity and a stress-based segregation criterion, enabling predictions of segregation from mechanical stress accumulation at interfaces rather than solely from energy minimization or local rules.

The morphology of migrating epithelial cells can be characterised by the coordination number of epithelial cells in contact with mesenchymal cells z_{em}. In this line, three regimes can be established: (i) low z_{em} corresponds to migration of higher-sized compact epithelial clusters or monolayer sheets, (ii) medium z_{em} corresponds to epithelial migration in the form of partially-connected supracellular network or open, irregularly-shaped clusters, and (iii) high z_{em} corresponds to migration of epithelial cells in the form of small clusters and single cells. Consequently, the biointerface area is smaller for lower z_{em}, while high z_{em} is characteristic of larger-sized biointerface areas.

The size of the biointerface influences the mechanical coupling between the subpopulations by influencing the energy transfer across the subpopulations, which can homogenize the distribution of mechanical stress to some extent. A decrease in the biointerface size leads to an increase in the degree of inhomogeneity in the distribution of stress within spheroids. Mechanical mismatch caused by an inhomogeneous distribution of mechanical stress, quantified by the gradient of macroscopic stress within the spheroid part, accompanied by the interfacial tension, has the potential to speed up the segregation process. The mechanical mismatch and the interfacial tension between the subpopulations are closely interconnected. The first one is a volumetric phenomenon, while the second is a surface phenomenon.

The effectiveness of the segregation process is determined by the divergence of the macroscopic stress within a spheroid and the contact dynamics at the biointerface between the subpopulations. It is therefore essential to quantify the mechanical coupling between them.

3.1 Macroscopic stress within a spheroid part: a theoretical analysis

Macroscopic stress within the spheroid depends on the viscoelasticity of the subpopulations caused by collective cell migration and heterotypic interactions along the biointerface. The epithelial–mesenchymal biointerface does not just passively transmit stress — it actively contributes to it by: (i) resisting deformation (via interfacial tension), (ii) allowing force transmission or shielding (depending on heterotypic adhesion), and (iii) remodelling dynamically (e.g., via changes in coordination number z_{em}), and (iv) its bending.

The gradient of the macroscopic stress $\vec{\nabla}\tilde{\boldsymbol{\sigma}}_{\boldsymbol{rT}}$ represents the driving force for the segregation process. Consequently, the macroscopic stress caused by the segregation of the subpopulations is influenced by:

- Change in the size of the biointerface area
- The local volume fraction of epithelial cells within a part of the spheroid characterized by a positional vector $\vec{\boldsymbol{r}} = r(x, y, z)$ expressed as: $\phi_e(r, \tau) = \langle V_e \rangle n_e$ and the local volume fraction of mesenchymal cells expressed as: $\phi_m(r, \tau) = \langle V_m \rangle n_m$ (where τ is a timescale of hours, $\langle V_e \rangle$ and $\langle V_m \rangle$ are the single-cell average volumes for epithelial cells and mesenchymal cells, respectively, $n_e(r, \tau)$ is the epithelial cell packing density, and , $n_m(r, \tau)$ is the mesenchymal cell packing density). The volume fractions satisfy the condition: $\phi_e + \phi_m = 1$.
- Residual stresses within the epithelial and mesenchymal subpopulations located at r within the spheroid (i.e., the stress that remains in the system) are influenced by: (i) the interfacial tension and interfacial tension gradient; and (ii) the viscoelasticity of the subpopulations described by one of the proper constitutive models discussed in **Box 1**.

Box 1. Residual stresses of the subpopulations

Residual stresses of the subpopulations consist of normal and shear stress components.

Normal residual stresses of the subpopulations include isotropic and deviatoric contributions. The isotropic contribution depends on the epithelial-mesenchymal interfacial tension γ_{em} and can be expressed based via the Young-Laplace equation as: $\Delta p_{m\to e} = -\gamma_{em}\kappa$ (where κ is the mean curvature of the biointerface expressed as: $\kappa = \frac{1}{2}\vec{\nabla}\left(\frac{\vec{\nabla}w}{\sqrt{1+|\vec{\nabla}w|^2}}\right)$ and w is the out-of plane displacement). The interfacial tension does work in reducing the biointerface area. This reduction leads to compression of one subpopulation and extension of the other (Pajic-Lijakovic et al., 2023b). The epithelial subpopulation is more cohesive than the mesenchymal one (Devanny et al., 2021; Pajic-Lijakovic et al., 2025b). The deviatoric contribution to the normal residual stress depends on the viscoelasticity of the subpopulations caused by collective cell migration. Consequently, the normal residual stress within the epithelial and mesenchymal subpopulations was expressed by Pajic-Lijakovic et al. (2025b) as:

$$\widetilde{\boldsymbol{\sigma}}_{\boldsymbol{rNi}}(r,\tau) = \pm\Delta p_{m\to e}\tilde{\boldsymbol{I}} + \widetilde{\boldsymbol{\sigma}}_{\boldsymbol{rNi}}^{\boldsymbol{CCM}}$$

where $i \equiv e, m$, with e for the epithelial subpopulation and m for the mesenchymal subpopulation, $\tilde{\boldsymbol{I}}$ is the unit tensor and $\widetilde{\boldsymbol{\sigma}}_{\boldsymbol{rNi}}^{\boldsymbol{CCM}}$ is the deviatoric contribution to the normal stress. The sign ''+'' in front of the first term indicates an extension of mesenchymal subpopulation, while the sign ''-'' points to compression of the epithelial subpopulation.

Shear residual stresses are generated actively via collective cell migration and passively via the gradient of the interfacial tension (Pajic-Lijakovic et al., 2025b). Inhomogeneous distribution of the interfacial tension is caused by the inhomogeneous nature of homotypic and heterotypic cell-cell interactions. Cell movement along the biointerface from the region of lower to higher interfacial tension is known as the Marangoni effect (Gsell et al., 2023; Pajic-Lijakovic et al., 2025b). Similar effects have been recognized in various soft matter systems (Karbalaei et al., 2016). Consequently, the shear stress within the subpopulations was expressed as (Pajic-Lijakovic et al., 2025b):

$$\vec{\boldsymbol{n}}\cdot\widetilde{\boldsymbol{\sigma}}_{\boldsymbol{rSi}}(r,\tau)\cdot\vec{\boldsymbol{t}} = \vec{\boldsymbol{\nabla}}_{\boldsymbol{s}}\gamma_{em}\cdot\vec{\boldsymbol{t}} + \vec{\boldsymbol{n}}\cdot\widetilde{\boldsymbol{\sigma}}_{\boldsymbol{rSi}}^{\boldsymbol{CCM}}\cdot\vec{\boldsymbol{t}}$$

where $i \equiv e, m$, $\widetilde{\boldsymbol{\sigma}}_{\boldsymbol{rSi}}(r,\tau)$ is the cell shear residual stress, $\widetilde{\boldsymbol{\sigma}}_{\boldsymbol{rSi}}^{\boldsymbol{CCM}}$ is the shear stress generated by collective cell migration, $\vec{\boldsymbol{n}}$ is the unit vector normal to the biointerface, and $\vec{\boldsymbol{t}}$ is the tangential unit vector along the biointerface.

The **residual stresses caused by collective cell migration** of epithelial and mesenchymal subpopulations $\widetilde{\boldsymbol{\sigma}}_{\boldsymbol{ri}}^{\boldsymbol{CCM}}$ depend on the viscoelasticity of the subpopulations. The viscoelasticity is influenced by the cumulative effects of cell contractions and the strength of homotypic cell-cell adhesion contacts. The migration of mesenchymal cells is more dissipative than that of epithelial cells and has been treated in terms of a viscoelastic liquid. In contrast to the mesenchymal subpopulation, the migrating epithelial collectives behave as a viscoelastic solid. The dissipative nature of the migration of mesenchymal collectives prevents accumulation of compressive stress accompanied by an increase in the packing density within bulk regions. Increase in the packing density of mesenchymal cells can be significant only near the biointerface (Guan et al., 2023). In contrast to mesenchymal cells, migration of epithelial cells leads to intensive accumulation of compressive stress accompanied by an increase in the epithelial packing density (Notbohm et al., 2016; Tlili et al., 2018). Epithelial cells tend to maintain strong cell-cell adhesion contacts when subjected to an increased cell packing density, approaching a state near jamming. Viscoelasticity of the subpopulations was discussed in the context of various constitutive models proposed in agreement with experimental findings by Serra-Picamal et al. (2012), Notbohm et al., 2016, Marmottant et al. (2009), and Tlili et al. (2018).

Viscoelasticity of epithelial subpopulation caused by collective cell migration

Various mechanisms of energy dissipation during rearrangement of epithelial cells primarily depend on epithelial packing density n_e. In this context three regimes can be distinguished: (i) regime 1: $n_e \leq n_{conf}$, (ii) regime 2: $n_{conf} < n_e < n_j$ (where n_{conf} is the cell packing density in the confluent state and n_j is the cell packing density in the jamming state) and (iii) regime 3: $n_e \to n_j$. The main characteristics of these regimes in the context of energy dissipation are (Pajic-Lijakovic et al., 2025a):

- **Regime 1**: Energy dissipation within the epithelial subpopulation arises through a remodeling of cell-cell adhesion contacts, which occurs over minutes (Lee and Wolgemuth, 2011; Pajic-Lijakovic et al., 2025b). It ensures a relaxation of stress. Under these conditions, the epithelial subpopulation retains ordered, anisotropic trends of migration. The corresponding mechanism of cell migration is convective. The Zener constitutive model, suitable for viscoelastic solids, has been used for describing the viscoelasticity of migrating epithelial collectives (**Appendix**). Its main characteristic is that stress can relax toward the residual stress within a few minutes (Marmottant et al., 2009; Khalilgharibi et al., 2019). Consequently, the stress relaxes within many short-time relaxation cycles under constant strain per cycle, while the strain and residual stress increase slowly over hours. The residual stress is elastic. Zhao et al. (2013) also treated multicellular systems as elastic.
- **Regime 2**: An increase in epithelial packing density leads to a change in the mechanism of energy dissipation. In this case, cell-cell interactions, intensive under higher cell packing density, perturb cell alignment leading to a decrease in the degree of anisotropy, causing energy dissipation over hours. The underlying mechanism of cell migration is diffusive. Stress cannot relax. Consequently, the linear constitutive model, suitable for viscoelastic solids, for the higher packing density of epithelial cells is the Kelvin-Voigt model (**Appendix)**. The corresponding cell residual stress includes both elastic and viscous contributions.
- **Regime 3**: Intensive cell-cell interactions near jamming lead to contact inhibition of locomotion (CIL). The CIL includes weakening of cell-cell and cell-matrix adhesion contacts during the process of cell repolarization (Roycraft and Mayor, 2016). The mechanism of cell migration in this case is nonlinear and sub-diffusive, while the energy dissipation occurs over hours. In accordance with fact that fractional derivatives have been used for describing damped, sub-diffusive migration of epithelial cells, Pajic-Lijakovic and Milivojevic (2021) proposed the Fractional constitutive model to describe epithelial cells near jamming (**Appendix)**.

Viscoelasticity of mesenchymal subpopulation caused by collective cell migration

While, the dissipative nature of epithelial residual stress is pronounced under higher cell packing density, residual stress of the mesenchymal subpopulation is purely dissipative even at lower cell packing density (i.e., cell packing density $n_e \leq n_{conf}$). Viscoelasticity of the mesenchymal subpopulation caused by collective cell migration was described by the Maxwell model, suitable for viscoelastic liquids (**Appendix)**. The main characteristic of this model is that stress can relax under constant strain rates within a few minutes, while the residual stress changes over hours. Consequently, the stress changes within successive short-time relaxation cycles under constant strain rate per cycle, while the strain rate changes over hours. The residual stress is purely dissipative.

Although the constitutive behavior of epithelial and mesenchymal subpopulations is addressed in the existing literature, the influence of the dynamics along the biointerface on the constitutive behaviour of co-cultured epithelial-mesenchymal spheroids, and the generation of macroscopic stress, has not been as thoroughly examined. Furthermore, it is important to highlight the effect of the biointerface on the

mechanical stress by including the mechanical coupling between the subpopulations. In this context, the macroscopic stress can be expressed as:

$$\widetilde{\boldsymbol{\sigma}}_{\boldsymbol{rT}}(r,\tau) = \phi_e \widetilde{\boldsymbol{\sigma}}_{\boldsymbol{r\,e}} + (1-\phi_e)\widetilde{\boldsymbol{\sigma}}_{\boldsymbol{r\,m}} + \widetilde{\boldsymbol{\sigma}}_{\boldsymbol{int}} \quad (1)$$

where $\widetilde{\boldsymbol{\sigma}}_{\boldsymbol{r\,e}}$ is the epithelial residual stress, $\widetilde{\boldsymbol{\sigma}}_{\boldsymbol{r\,m}}$ is the mesenchymal residual stress, and $\widetilde{\boldsymbol{\sigma}}_{\boldsymbol{int}}$ is the stress along the biointerface which is given by:

$$\widetilde{\boldsymbol{\sigma}}_{\boldsymbol{int}} = \frac{1}{l_{int}}\gamma_{em}\widetilde{\boldsymbol{P}} + \frac{1}{2}\left(\vec{\boldsymbol{\nabla}}_{\boldsymbol{s}}\gamma_{em} \otimes \vec{\boldsymbol{t}} + \vec{\boldsymbol{t}} \otimes \vec{\boldsymbol{\nabla}}_{\boldsymbol{s}}\gamma_{em}\right) \quad (2)$$

where $\widetilde{\boldsymbol{P}}$ is the projection tensor onto the tangent plane of the interface equal to: $\widetilde{\boldsymbol{P}} = \tilde{\boldsymbol{I}} - \vec{\boldsymbol{n}} \otimes \vec{\boldsymbol{n}}$ and l_{int} is the average thickness of the biointerface. The first term on the right-hand side of eq. 2 is isotropic, while the second term accounts for inhomogeneity of the interfacial tension. When the biointerface is not sharp, primarily due to the epithelial-to-mesenchymal transition, an additional contribution to the interfacial stress is needed: $\Delta\widetilde{\boldsymbol{\sigma}}_{\boldsymbol{int}} = \gamma_{em}\left(\vec{\boldsymbol{\nabla}}\phi_e \otimes \vec{\boldsymbol{\nabla}}\phi_e\right)$**.** Mechanical coupling between the subpopulations depends on the area of the biointerface. The mechanical coupling was formulated by Takaynagi et al. (1964) in order to describe the viscoelasticity of two-phase polymer blends. An increase in the biointerface area between polymer phases causes homogenization of the mechanical stress within them. This general statement can be applied here to the coupling between the cell subpopulations and formulated as:

$$\widetilde{\boldsymbol{\sigma}}_{\boldsymbol{r\,e}} - \widetilde{\boldsymbol{\sigma}}_{\boldsymbol{r\,m}} = f(A)\widetilde{\boldsymbol{D}} \quad (3)$$

where the initial stress difference is equal to $\widetilde{\boldsymbol{D}} = \widetilde{\boldsymbol{\sigma}}_{\boldsymbol{r\,e}}{}^{\infty} - \widetilde{\boldsymbol{\sigma}}_{\boldsymbol{r\,m}}{}^{\infty}$**,** $\widetilde{\boldsymbol{\sigma}}_{\boldsymbol{r\,e}}{}^{\infty}$ and $\widetilde{\boldsymbol{\sigma}}_{\boldsymbol{r\,m}}{}^{\infty}$ are bulk stresses of the epithelial and mesenchymal subpopulations at the end of the segregation process, $f(A)$ is a decreasing function of interface area $A(\tau)$ during the segregation process that could be approximated as: $f(A) = e^{-k_A(A-A_\infty)}$, k_A is a measure of the increase in stress difference caused by a decrease in the biointerface area, and A_∞ is the area of the biointerface at the end of the segregation process.

The area of the biointerface decreases during the segregation process. In the initial regime, the process is driven primarily by the epithelial-mesenchymal interfacial tension and the interfacial tension gradient, while the stress is more homogeneously distributed within the spheroid. However, in the later regime, the segregation speeds up, being additionally driven by the divergence of macroscopic stress within the spheroid, which is a consequence of the mechanical coupling of the subpopulations. The efficiency of the segregation in the spheroid can be defined as: $S(r,\tau) = \int_v (\phi_e(r,\tau) - \langle\phi_e\rangle)^2 dV$ (where $\langle\phi_e\rangle$ is the average volume fraction of epithelial cells within the spheroid). When $S(r,\tau) = 0$, the two subpopulations are totally mixed. The efficiency $S(r,\tau)$ increases during the segregation process towards the equilibrium value S_{eq} that corresponds to partial or complete segregation. The rate of change of the efficiency $S(r,\tau)$ is $R_S = \frac{dS}{d\tau}$. Changes in the volume fraction of epithelial cells within the spheroid can be expressed as:

$$\frac{\partial\phi_e}{\partial\tau} + \vec{\boldsymbol{\nabla}} \cdot \vec{\boldsymbol{J}}_{\boldsymbol{e}}^{\boldsymbol{M}} = 0 \quad (4)$$

where $\vec{\boldsymbol{j}}_{\boldsymbol{e}}^{\boldsymbol{M}}$ is the macroscopic flux $\vec{\boldsymbol{j}}_{\boldsymbol{e}}^{\boldsymbol{M}} = -D_M\vec{\boldsymbol{\nabla}}\phi_e + K_c\phi_e(1-\phi_e)\nabla\tilde{\boldsymbol{\sigma}}_{\boldsymbol{rT}}$, D_M is the macroscopic diffusion coefficient of the epithelial subpopulation, and K_c is the coupling coefficient of the subpopulations. The efficiency of segregation increases with: (i) divergence of macroscopic stress $\nabla\tilde{\boldsymbol{\sigma}}_{\boldsymbol{rT}}$, (ii) intermediate mixing $\phi_e(1-\phi_e)$, (iii) gradient of the volume fraction of the epithelial subpopulation, and (iv) an increase in the mechanosensitivity quantified by the coefficient K_c. It is important to emphasize the significance of contact dynamics between the subpopulations along the biointerface in relation to the distribution of residual stress within the spheroid.

4. Contact dynamics along the biointerface

The biointerface is characterized by the position vector: $\vec{\boldsymbol{\Re}} = \Re(X,Y,Z))$ (where X,Y,Z are the coordinates of the biointerface, and $Z = w(X,Y)$ is the out-of-plane displacement due to bending of the biointerface). The referent (undeformed) state of the biointerface can be characterised as $\Re_0(X,Y,0)$. The coordinates of the biointerface can be correlated with the coordinates within a spheroid of the form: $\vec{\boldsymbol{r}} = \vec{\boldsymbol{\Re}} + \xi\vec{\boldsymbol{n}}$ (where ξ is the distance from the biointerface and $\vec{\boldsymbol{n}}$ is the unit vector normal to the biointerface at the point $\Re(X,Y,Z)$). We suppose that clusters of epithelial cells are much larger than the size of single cells and that contact dynamics along the biointerface can be discussed in the context of continuum mechanics.

Taking account of the biointerface's mechanical deformation and changes in its area caused by collective migration of the epithelial and mesenchymal subpopulations, the energy contributions along the biointerface are:

(i) the strain energy, which is equal to $e_{es}(\Re,t,\tau) = \Delta V_{\Re}(\tilde{\boldsymbol{\sigma}}_{\boldsymbol{e}}:\tilde{\boldsymbol{\varepsilon}}_{\boldsymbol{e}} + \tilde{\boldsymbol{\sigma}}_{\boldsymbol{m}}:\tilde{\boldsymbol{\varepsilon}}_{\boldsymbol{m}})$ (where $\Delta V_{\Re}$ is the volume of perturbed biointerface at $\Re$, $\tilde{\boldsymbol{\varepsilon}}_{\boldsymbol{e}}$ and $\tilde{\boldsymbol{\varepsilon}}_{\boldsymbol{m}}$ are epithelial and mesenchymal strains)

(ii) the Helfrich type of bending energy, which can be expressed as: $e_{eb} = \frac{1}{2}E_b\left(\frac{\partial^2}{\partial x^2}w + \frac{\partial^2}{\partial y^2}w - 2C_0\right)^2 + E_b^G\left(\frac{\partial^2}{\partial x^2}w\frac{\partial^2}{\partial y^2}w - \left(\frac{\partial^2}{\partial x\partial y}w\right)^2\right)dA$ (Audoly and Pomeau, 2010) (where E_b is the bending modulus, which is space-time dependent for viscoelastic epithelial multicellular systems, E_b^G is the Gaussian bending modulus, C_0 is the spontaneous curvature, and A is the surface area of the biointerface) (Audoly and Pomeau, 2010), and

(iii) the surface energy is $e_{em} = \gamma_{em}dA$.

While the epithelial and mesenchymal strains within the bulk regions of the subpopulations (i.e., the clusters of the subpopulations) are linear, the strains of the subpopulations along the biointerface are rather nonlinear on account of: (i) the biointerface's bend and fold, (ii) the large deformation gradient caused by movement of the subpopulations in opposite directions, and (iii) the mechanical mismatch induced by differences in the viscoelasticity of the subpopulations. Consequently, the epithelial strain is $\tilde{\boldsymbol{\varepsilon}}_{\boldsymbol{e}}(\Re,\tau) = \frac{1}{2}\left(\vec{\boldsymbol{\nabla}}\vec{\boldsymbol{u}}_e + \vec{\boldsymbol{\nabla}}\vec{\boldsymbol{u}}_e^{\,\boldsymbol{T}} + (\vec{\boldsymbol{\nabla}}\vec{\boldsymbol{u}}_e)^{\boldsymbol{T}}\vec{\boldsymbol{\nabla}}\vec{\boldsymbol{u}}_{\boldsymbol{e}}\right)$, while the mesenchymal strain is $\tilde{\boldsymbol{\varepsilon}}_{\boldsymbol{m}}(\Re,\tau) = \frac{1}{2}\left(\vec{\boldsymbol{\nabla}}\vec{\boldsymbol{u}}_m + \vec{\boldsymbol{\nabla}}\vec{\boldsymbol{u}}_m^{\,\boldsymbol{T}} + (\vec{\boldsymbol{\nabla}}\vec{\boldsymbol{u}}_m)^{\boldsymbol{T}}\vec{\boldsymbol{\nabla}}\vec{\boldsymbol{u}}_{\boldsymbol{m}}\right)$.

The epithelial-mesenchymal interactions along the biointerface can be discussed in the context of the coordination number of epithelial cells in contact with surrounding mesenchymal cells z_{em} which is correlated with: (i) the distance between the subpopulations along the biointerface caused by interplay between heterotypic attraction and repulsion, (ii) the epithelial-mesenchymal interfacial tension, (iii) the area of the biointerface, and (iv) the epithelial and mesenchymal packing density along the biointerface.

4.1 Coordination number of an epithelial cell in contact with mesenchymal cells

A topological constraint for an individual epithelial cell dictates that it must be coordinated either with neighbouring epithelial cells, or with mesenchymal cells (or with a combination of them). When an epithelial cell is located at the biointerface, the coordination number z_{em} is $z_{em} \geq 1$. In contrast, when the coordination number $z_{em} = 0$, the epithelial cell is located within the bulk region of an epithelial cluster. When an epithelial cell migrates as a single cell surrounded by mesenchymal cells, $z_{em} = z^*$ (where z^* is the maximum coordination number of epithelial cells in contact with mesenchymal cells), but it is rare event. The contact dynamics between epithelial and mesenchymal subpopulations discussed in the context of the coordination number z_{em} is shown in **Figure 2**:

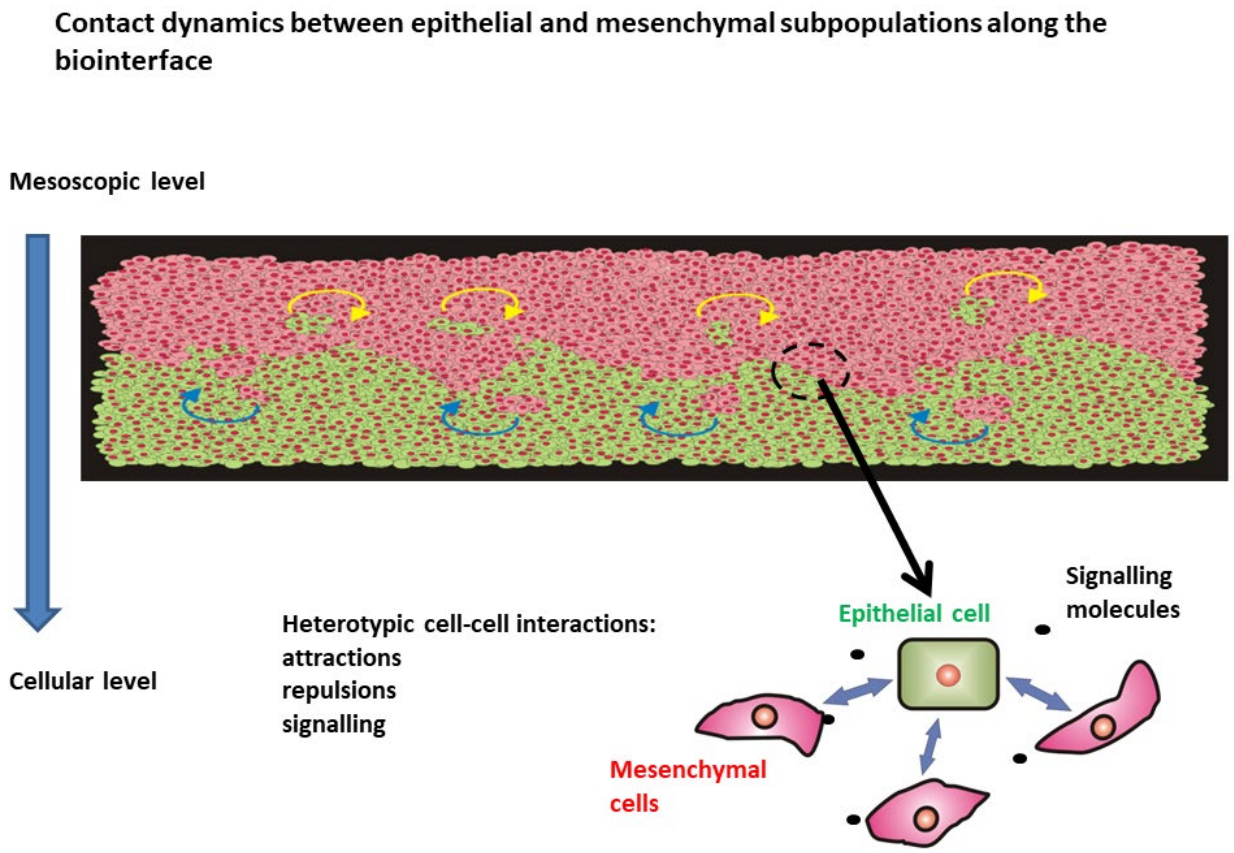

Figure 2. Contact dynamics between the epithelial and mesenchymal subpopulations: from mesoscopic to cellular levels, was considered in the context of the coordination number z_{em} by pointing to heterotypic cell-cell interactions.

The coordination number z_{em} changes via collective cell migration over hours. Segregation and coordinated migration between epithelial and cancer mesenchymal-like cells are governed by a combination of contact-dependent adhesion, paracrine EMT signals, chemokines, mechanotransduction pathways, and ECM-mediated cues. Differential expression of cadherins (E- versus N-cadherin) and Eph/ephrin signaling regulates interfacial tension and boundary formation, while TGF-β, Wnt/β-catenin, and Notch pathways promote mesenchymal-like phenotypes and motility. Mechanosensitive pathways, including Rho–ROCK, myosin II, and YAP/TAZ, convert tissue-level stresses into biochemical responses, reinforcing segregation and collective rearrangements. Interactions with the extracellular matrix via integrins, fibronectin, collagen, and MMP-mediated remodeling further bias spatial organization and migration dynamics. Collectively, these signals operate at the cell–cell and cell–matrix interfaces, coordinating multicellular behavior and stabilizing domain formation in mixed spheroids (Mierke, 2019; Mierke, 2024; Kabla, 2012). Small extracellular vesicles originating from breast mesenchymal-like MDA-MB-231 cells enhance the proliferation and motility of breast cancer epithelial-like MCF7 cells (Senigagliesi et al., 2022). The breast epithelial MCF10A cells produce laminin-5 and fibronectin, which in turn activate focal adhesions (FAs) in cancer cells like the MDA-MB-231 cells, potentially enhancing their motility (Nikkhah et al., 2011).

The contact dynamics between the subpopulations at a cellular level was discussed earlier in the form of a Langevin-type equation (Pajic-Lijakovic et al. (2025b) as:

$$\frac{\partial z_{em}}{\partial \tau} = -\mu_e \frac{\partial U_{int}}{\partial z_{em}} + \sqrt{D(z_{em})}\Gamma \tag{5}$$

where μ_e is the mobility of epithelial cells along the biointerface, U_{int} is the interaction potential at a cellular level discussed in the **Section 4.2**, and Γ is white noise.

The coordination number z_{em} can be correlated with the distance between epithelial and mesenchymal cells d_{em}. The distance d_{em} is the main parameter that governs attraction/repulsion between the subpopulations such that: (i) attraction is dominant for the case of $d_{em} > d_0$ and (ii) repulsion is dominant for the case of $d_{em} \leq d_0$ (where d_0 is a characteristic distance $d_0 \sim 8\,\mu\text{m}$, Deforet et al. (2014)). The correlation between these two parameters can be formulated by introducing the cutoff radius R_c, which describes the space with the number of mesenchymal cells per single epithelial cell along the biointerface. Consequently, the number density of mesenchymal cells in contact with a single epithelial cell is equal to $\frac{z_{em}}{\frac{4}{3}\pi R_c^3}$.

The evolution of the distribution ρ_a of the coordination numbers z_{em} was expressed in the form of a Fokker-Planck equation by the modified model proposed by Pajic-Lijakovic et al. (2025b) as:

$$\frac{\partial \rho_a(z_{em},\tau)}{\partial \tau} = -\frac{\partial}{\partial z_{em}}\left[\frac{\partial U_{int}(z_{em})}{\partial z_{em}}\rho_a\right] + \frac{\partial^2}{\partial {z_{em}}^2}[D_z(z_{em})\rho_a] \tag{6}$$

where $\frac{\partial U_{int}(z_{em})}{\partial z_{em}}$ is the rate of change of z_{em} and $D(z_{em}) = \frac{\langle(\Delta z_{em})^2\rangle}{\Delta\tau}$ is the rate of variance growth The rate of change z_{em} can be expressed by formulating the epithelial-mesenchymal interaction potential $U_{int}(z_{em})$. A minimum of $U_{int}(z_{em})$ at a preferred number of mesenchymal contacts can reflect a stable interfacial configuration. Macroscopic parameters such as fraction of interfacial epithelial cells and fraction of bulk epithelial cells can be calculated by using the distribution function ρ_a. Consequently, the fraction of interfacial epithelial cells $f_{eS}(\tau)$, which have at least one contact with mesenchymal cells can be calculated from the distribution $\rho_a(z_{em},\tau)$ as: $y_{eS}(\tau) = \int_1^{z^*} \rho_a(z_{em},\tau) d\, z_{em}$ (where $\rho_a(z_{em},\tau)$ is the distribution of coordination numbers z_{em} of epithelial cells). The fraction of epithelial cells located within the bulk of the epithelium is $y_{eV}(\tau) = 1 - y_{eS}(\tau)$.

The contact dynamics between the subpopulations at a mesoscopic level can be discussed in the context of the average coordination number at the biointerface located at $\Re$, labelled as $\langle z_{em}\rangle^{\Re}$. This parameter can be correlated with the packing densities of the subpopulations and expressed as:

$$\langle z_{em}\rangle^{\Re} = \frac{n_m}{n_e} \tag{7}$$

where $n_e(\Re,\tau)$ is the packing density of epithelial cells, $n_m(\Re,\tau)$ is the packing density of mesenchymal cells along the biointerface, and τ is a time-scale of hours. This average coordination number accompanied by the packing densities of the subpopulations depends on the biointerface bending. Their interrelationship can be formulated as:

$$\langle z_{em}\rangle^{\Re}(\tau) = z_0 + \mu_1\left(\frac{\partial^2 w}{\partial x^2} + \frac{\partial^2 w}{\partial y^2}\right) + \mu_2\left[\frac{\partial^2 w}{\partial x^2}\frac{\partial^2 w}{\partial y^2} - \left(\frac{\partial^2 w}{\partial x \partial y}\right)^2\right] \tag{8}$$

where z_0 is the average coordination number for a flat biointerface, w is the out-of-plane displacement, μ_1 quantifies sensitivity to mean curvature such that $\mu_1 < 0$ for concave curvatures and $\mu_1 > 0$ for convex curvatures, and μ_2 quantifies sensitivity to Gaussian curvature. While concave curvatures decrease the coordination number $\langle z_{em}\rangle^{\Re}$, convex curvatures increase $\langle z_{em}\rangle^{\Re}$. On concave biointerfaces, epithelial cells are compressed and packed closely with one another, which reduces the portion of their surface exposed to mesenchymal neighbors, leading to a decrease in $\langle z_{em}\rangle^{\Re}$. Conversely, on convex surfaces, epithelial cells are stretched and flattened along the biointerface, increasing the area available for contact with mesenchymal cells, so that $\langle z_{em}\rangle^{\Re}$ increases. Therefore, surface curvature modulates epithelial–mesenchymal interactions by altering the exposed biointerfacial area of epithelial cells, with convex regions favouring higher mesenchymal coordination and concave regions reducing it.

In further consideration, it is necessary to formulate the interaction potential $U_{int}(d_{em}, z_{em})$ between the subpopulations as functions of the correlation number z_{em} and the average distance d_{em}. The interaction potential influences the distribution of the coordination number z_{em} which has a feedback impact on: (i) the interfacial tension, (ii) the area of the biointerface, and (iii) the relationship between them.

4.2 The interaction potential between epithelial and mesenchymal cells along the biointerface

The interaction potential accounts for the attractive, repulsive, and signalling interactions between epithelial and mesenchymal cells that contribute to their mechanical coupling. Attractive and repulsive parts of the potential have been expressed in the form of the Lennard-Jones potential (Kang et al., 2021). Consequently, the interaction potential per single epithelial cell can be formulated as:

$$U_{int}(d_{em}, z_{em}) = z_{em} U_{vdW}(d_{em}) + U_{sig}(z_{em}) \quad (9)$$

where U_{vdW} is the van der Waals potential that accounts for many body interactions (Israelachvili, 2011) and can be expressed as: $U_{vdW} = \sum_{i<j} U_2(i,j) + \sum_{i<j<k} U_3(i,j,k) + \cdots$, $U_2(i,j)$ is the two-body potential, $U_3(i,j,k)$ is the three-body potential, and $U_{sig}(z_{em})$ is the contribution to the interaction potential caused by cell signalling. Van der Waals (vdW) potentials are frequently used to describe molecular interactions, including both attractive and repulsive contributions (Tkatchenko et al., 2012; Hingangavkar, 2025). Hauseux et al. (2022) and Sosa et al. (2025) pointed out that many-body descriptions of van der Waals interactions — beyond simple pairwise models — can simulate force responses far stronger than expected from two-body interactions. Attractive interactions result from intermolecular forces, such as London dispersion, while repulsive interactions prevent overlap at very short distances. Shen et al. (2025) developed machine learning surrogate models for predicting many-body dispersion (MBD) interactions, enabling efficient incorporation of complex van der Waals forces into large-scale simulations. Because many-body dispersion represents a collective extension of pairwise interaction models, the paper from Shen et al. (2025) provides a contemporary example of how complex, non-pairwise vdW-related forces can be modeled and approximated in computational settings.

At the cellular scale, vdW-inspired potentials treat effective cell–cell interactions similarly: adhesion and cohesion are represented by attractive terms, and steric, cortical, or electrostatic barriers by repulsive terms, allowing modeling of intercellular spacing and tissue cohesion. The two-body potential can be expressed in the form of the Lennard-Jones potential describing attraction/repulsion per single heterotypic contact, i.e. $U_2(i,j) \equiv U_{LJ}$. The Lennard-Jones potential can be expressed as: $U_{LJ}(d_{em}) = e_r \left(\frac{d_0}{d_{em}}\right)^p - e_a \left(\frac{d_0}{d_{em}}\right)^q$, where e_a is the average attractive energy per single heterotypic contact, e_r is the average repulsive energy per single epithelial-mesenchymal contact, d_0 is the equilibrium distance between cells at which the attractive and repulsive forces exactly balance, and p, q are the scaling exponents. The interaction potential caused by cell signalling can be expressed as: $U_{sig}(z_{em}) = -e_s \varphi(z_{em})$ (where e_s is the energy contribution per unit signalling interaction between epithelial and mesenchymal cells and $\varphi(z_{em})$ acts as a functional bridge between cell-level contact geometry and signalling-driven state changes). The function $\varphi(z_{em})$ should account for: (i) the cooperativity of signalling that captures multiple contact sites thereby amplifying the signalling, (ii) thresholding that reflects the epithelial-to-mesenchymal transition (EMT) as a switch-like event when sufficient heterotypic contacts are reached, and (iii) saturation that models the limited receptor availability—the signal plateaus at high contact number (Cieślik et al., 2013). Accordingly, the Hill-type function $\varphi(z_{em})$ can be expressed as: $\varphi(z_{em}) = \frac{z_{em}^n}{K + z_{em}^n}$ (where n is the Hill coefficient often in the range of 2-6, and K is

the half-maximal coordination number). When z_{em} is $z_{em} \ll K$, then $S(z_{em}) \sim z_{em}$. Otherwise, when $z_{em} \gg K$ then $\varphi(z_{em}) \sim const$.

Attractive interactions between the epithelial and mesenchymal subpopulations result in the generation of adhesion energy between them. This energy depends on whether cells form direct heterotypic adhesion contact, ECM-mediated adhesion contacts or do not establish adhesion contacts. Even when cells do not establish adhesion contacts, adhesion energy between them arises as a result of the geometric confinement of cells. Geometric confinement refers to the physical restriction of cells within a defined space, such as a curved or small cavity, narrow channel, or dense tissue microenvironment. From a cell biological perspective, this confinement limits the space available for cell spreading, protrusion formation, and rearrangement, effectively controlling how cells can contact neighbours or migrate. Although it is purely mechanical/physical and not mediated by molecular adhesion molecules, it can mimic the effects of interfacial adhesion by creating an energy-like barrier: cells must deform, generate traction, or reorganize cytoskeletal and junctional structures to overcome the spatial restriction. In this sense, confinement behaves like an effective interfacial energy barrier, because it restricts cell motion or cell–cell rearrangements similarly to how actual biochemical adhesion (e.g., cadherin-mediated contacts) would resist detachment or interface rearrangement. This confinement may: (i) prevent detachment or rearrangement of cells along the biointerface, (ii) influence epithelial shape and motility, and (iii) require energy to break free, similar to pulling apart a physical adhesive contact. The primary mechanism related to the repulsive term in the Lennard-Jones potential is contact inhibition of locomotion (CIL), which depends on the coordination number z_{em} (Roycraft and Mayor, 2016).

The interaction potential influences the epithelial-mesenchymal interfacial tension and consequently the residual stresses within the subpopulations.

4.3 The impact of the interaction potential on epithelial-mesenchymal interfacial tension

The epithelial-mesenchymal interfacial tension γ_{em} contributes to the generation of normal stress within the subpopulations, while the gradient of the interfacial tension is responsible for the generation of shear stress along the biointerface. This parameter is space-time dependent. The interfacial tension can be expressed as (Pajic-Lijakovic et al., 2025b):

$$\gamma_{em}(\Re, \tau) = \gamma_e + \gamma_m + u_{int} \quad (10)$$

where γ_e and γ_m are the surface tensions of epithelial and mesenchymal subpopulations in contact with liquid medium (i.e., culture medium), the interaction potential per unit of the biointerface area $u_{int}(\Re, \tau) = \sum_i \delta(\Re_i - \Re)\, U_{int\, i}$, and $U_{int\, i}$ is the contribution to interaction potential per single cell. The interaction potential u_{int} can be: (i) $u_{int} < 0$ for attractive interactions and (ii) $u_{int} > 0$ for repulsive interactions. An attractive potential stabilises the biointerface by decreasing the interfacial tension γ_{em}, while a repulsive potential destabilises it by increasing the interfacial tension (Pajic-Lijakovic et al., 2025b).

The cohesion of epithelial multicellular surfaces is significantly higher than that of mesenchymal surfaces due to stronger homotypic cell-cell adhesion contacts (Devanny et al., 2021). Consequently, the surface tension of epithelial cells in contact with liquid medium is much higher than the surface tension of mesenchymal cells, i.e., $\gamma_e \gg \gamma_m$. Accordingly, the interfacial tension can be expressed as: $\gamma_{em}(\Re, \tau) = \gamma_e + u_{int}$.

The epithelial surface tension γ_e is affected by various factors, such as the contractility of cells, the adhesive strength of homotypic cell-cell interactions, and the deformation (i.e., stretching or compression) of multicellular surfaces (Devanny et al., 2021; Guevorkian et al., 2021; Pajic-Lijakovic et al., 2023a). The contractility of epithelial cells enhances the strength of homotypic cell-cell adhesion contacts leading to an increase in the epithelial surface tension (Devanny et al., 2021). While extension causes an increase in the epithelial surface tension (Guevorkian et al., 2021), compression intensifies the cell-cell interactions resulting in a decrease in the surface tension (Pajic-Lijakovic et al., 2023a).

The static tissue surface tension exhibits considerable variation across various cellular systems, ranging from a few $\frac{\mathrm{mN}}{\mathrm{m}}$ to several tens of $\frac{\mathrm{mN}}{\mathrm{m}}$ (Mombach et al., 2005; Stirbat et al., 2013; Nagle et al., 2022). However, it is difficult to estimate the variation of the epithelial surface tension along the biointerface without experimental data. We can discuss the variation of the surface tension of some soft matter systems such as water and collagen I film. For example, an increase in temperature from $0\ ^oC$ to $50\ ^{\mathrm{o}}\mathrm{C}$ induces a decrease in the surface tension of water of $7\ \frac{\mathrm{mN}}{\mathrm{m}}$. An increase in the collagen concentration from $1\ \frac{\mathrm{mg}}{\mathrm{ml}}$ to $4\ \frac{\mathrm{mg}}{\mathrm{ml}}$ causes the surface tension of a collagen film to decrease from $62\ \frac{\mathrm{mN}}{\mathrm{m}}$ to $57\ \frac{\mathrm{mN}}{\mathrm{m}}$ at $21\ ^{\mathrm{o}}\mathrm{C}$ (Kezwon and Wojciechowski, 2014).

The epithelial surface tension $\gamma_e(\Re, \tau)$ depends on the biointerface bending and can be expressed as (Binysh et al., 2022):

$$\gamma_e(\Re, \tau) = \gamma_{e0} + \gamma_H \kappa \qquad (11)$$

where γ_{e0} is the in-plane epithelial surface tension for a flat biointerface characterised by $\kappa \approx 0$, and γ_H is a measure of the sensitivity of the epithelial surface tension to a change of curvature. The concave shape of the biointerface from the side of epithelial subpopulation (i.e. $\kappa < 0$), which corresponds to local epithelial extension, leads to an increase in the surface tension γ_e, while a convex biointerface (i.e. $\kappa > 0$) corresponds to local compression of the biointerface leading to a decrease in γ_e.

As a result, the interfacial tension is influenced by: (i) the curvature associated with the epithelial surface tension and (ii) the coordination number z_{em} along with the distance d_{em} as determined by the interaction potential. The macroscopic epithelial surface tension $\gamma_e(\tau) = \frac{1}{\Delta A}\int_{\Omega} \gamma_e\,(\Re, \tau) d^2\Re$. The epithelial surface tension plays a significant role in decreasing the area of multicellular surface during: (1) the compaction of epithelial spheroids (Devanny et al., 2021), (2) the rounding of cell aggregates subjected to uni-axial compression (Mombach et al., 2005), (3) the de-wetting of cell aggregates on rigid surfaces (Beaune et al., 2018), and (4) the fusion of epithelial cell aggregates (Pajic-Lijakovic and Milivojevic, 2024a). An increase in the rate of change of the surface area of cell aggregates leads to a rise

in surface tension (Guevorkian et al., 2021). Based on these findings, a suitable constitutive model for dilation viscoelasticity was proposed by Pajic-Lijakovic et al. (2023b). It can be expressed at a macroscopic level as:

$$\Delta\gamma_e(\tau) = E_S \frac{\Delta A}{A_0} + \eta_S \frac{d}{d\tau}\left(\frac{\Delta A}{A_0}\right) \quad (12)$$

where $\Delta\gamma_e(\tau) = \gamma_e(\tau) - \gamma_e(0)$, E_S is the surface modulus of elasticity, and η_S is the surface viscosity. In further consideration, it is necessary to formulate the size of the biointerface area as a function of the distribution of the coordination number z_{em}.

4.4 An inhomogeneous distribution of the interfacial tension

An inhomogeneous distribution of interfacial tension is induced by inhomogeneous distributions of the coordination number z_{em}, the distance between the subpoplations d_{em}, the curvature κ, and the strength of heterotypic adhesion contacts, as well as by diffusion of the signalling molecules. Heterogeneity arising from cell signalling has been examined in two contexts: (1) cells within the same population reacting to distinct signals and/or (2) varied behaviours that can arise in response to identical signals (Blanchard et al, 2019; Petrungaro et al., 2019). The inhomogeneous distribution of interfacial tension also contributes to an inhomogeneous distribution of mechanical stress within the subpopulations along the biointerface. The gradient of mechanical stress within the epithelial subpopulation, in the form of a stiffness gradient, has a feedback impact on the migration of mesenchymal cells.

Inhomogeneous distributions of the interfacial tension between the placode and neural crest subpopulations in Xenopus embryos results from the establishment of unstable, transient heterotypic cell-cell adhesion contacts, as elaborated by Barriga et al. (2018). Furthermore, collective durotaxis has been documented in vivo in Drosophila and zebrafish embryos (Le and Mayor, 2023). Consequently, heterotypic cell-cell interactions and signalling, expressed through an interaction potential, are essential physical factors that create the mobile stiffness gradient within the placode boundary layer at the biointerface (Le and Mayor, 2023). Heterotypic repulsion interactions along the biointerface contribute to: (i) the extrusion of cancer-mesenchymal cells along the biointerface with the epithelial subpopulation and (ii) the segregation of co-cultured epithelial-mesenchymal monolayers (Guan et al., 2019; Lucia et al., 2022).

An inhomogeneous distribution of interfacial tension leads to the generation of a supracellular gradient of interfacial tension expressed as: $\vec{\nabla}_s \gamma_{em} = \frac{\Delta\gamma_{em}}{l}$ (where $\Delta\gamma_{em}$ is the difference in interfacial tension occurring at the tangential distance l along the flat biointerface). When the difference of interfacial tension $\Delta\gamma_{em} \sim 2 \frac{\mathrm{mN}}{\mathrm{m}}$ occurs at a distance $\sim 100\ \mu\mathrm{m}$, the corresponding shear stress contribution caused by the Marangoni effect is $20\ \mathrm{Pa}$. This is a large value, when we keep in mind that a shear stress of a few tens of Pa is capable of inducing inflammation of epithelial cells (Pitenis et al., 2018).

Given that: (i) interfacial tension changes the size of the biointerface area and (ii) change of the biointerface area significantly influences the mechanical coupling between the subpopulations, it is essential to articulate the biointerface area as function of epithelial cells, which are in contact with mesenchymal cells.

4.5 Changes of the biointerface area: the main factor influencing mechanical coupling between the subpopulations

The biointerface area $A(\tau)$ changes over hours via collective cell migration and was expressed (Pajic-Lijakovic et al., 2025b) as:

$$A(\tau) = y_{eS}(\tau) N_{Te} \langle A_{e\,eff} \rangle \quad (13)$$

where $y_{eS}(\tau)$ is the fraction of epithelial cells in contact with mesenchymal cells, $\langle A_e \rangle$ is the average surface area of a single epithelial cell in contact with mesenchymal cells, and N_{Te} is the total number of epithelial cells satisfying the condition that $N_{Te} \approx \text{const}$ during tissue self-organisation via collective cell migration. To gain a more profound understanding of dynamics at the biointerface, it is essential to establish mass and force balance equations for the various subpopulations.

5. Balance equations for epithelial and mesenchymal cells along the biointerface: a mesoscopic theoretical analysis

Mechanical coupling between the subpopulations influences the mass and force balances. It is in accordance with the fact that collective cell migration is more pronounced along the biointerface in comparison with bulk regions of the subpopulations. As a result, the formulation of mass and force balance equations constitutes a significant advance in comprehending the physical mechanisms underlying heterotypic cell-cell interactions.

5.1 Mass balance of epithelial and mesenchymal cells along the biointerface

The primary feature of epithelial collective migration is the inhomogeneous distribution of mechanical stress and cell packing density, whereas mesenchymal cells exhibit more uniform distributions of these physical parameters. This behavioural disparity between the two subpopulations is attributable mainly to the relative strengths of their cell-cell adhesion contacts. The migration mechanism of mesenchymal cells is characterized as convective, meaning that they move individually in a persistent and directional manner at a speed higher than that corresponding to a diffusion mechanism. This diffusion speed can be recognized in migrating epithelial collectives under higher cell packing density: $\|\vec{v}\|_D = D_{eff} \frac{1}{L_c}$ (where D_{eff} is the effective diffusion coefficient and L_c is the velocity correlation length) (Pajic-Lijakovic and

MIlivojevic, 2021). The effective diffusion coefficient decreases from $\sim 0.40\ \frac{\mu m^2}{\min}$ to $\sim 0.10\ \frac{\mu m^2}{min}$ when the packing density of MDCK cells increases from $\sim 1.40x10^5\ \frac{cells}{cm^2}$ to $\sim 2.63x10^5\ \frac{\text{cells}}{\text{cm}^2}$ (Angelini et al., 2011). The velocity correlation length depends on cell packing density and corresponds to a few tens of μm (Petrolli et al., 2021).

As a result, mesenchymal cell migration proves to be more effective than that of epithelial cells. The localized accumulation of compressive stress, coupled with an increase in cell packing density, leads to a transition in the migration mechanism of epithelial cells from convective to conductive (diffusive) and subsequently to sub-diffusive.

The mass balance of epithelial cells can be expressed in terms of a modified version of the model proposed by Pajic-Lijakovic et al. (2025b). We formulate here the contact-mediated motility flux and sink term caused by the EMT. The balance is expressed as:

$$\frac{dn_e}{d\tau} + \vec{\nabla} \cdot \vec{J}_e = S_{EMT} \tag{14}$$

where $\vec{J}_e$ is the flux of epithelial cells, which includes several contributions and can be expressed as: $\vec{J}_e = \vec{J}_e^{\,conv} + \vec{J}_e^{\,m} + \vec{J}_e^{\,mix}$, $\vec{J}_e^{\,conv}$ is the convective flux, which is valid for a cell packing density $n_e \leq n_{conf}$, $\vec{J}_e^{\,m}$ is the Marangoni flux, which depends on the gradient of interfacial tension $\vec{\nabla}_s \gamma_{em}$ (Pajic-Lijakovic et al., 2023b), and $\vec{J}_e^{\,cm}$ is the contact-mediated motility flux formulated here. While the Marangoni flux directs cell migration tangentially along the biointerface, the contact-mediated motility flux causes cell migration in both the normal and tangential directions. The convective flux of epithelial cells can be expressed as: $\vec{J}_e^{\,conv} = n_e \vec{v}_e$ (where $\vec{v}_e$ is the velocity of epithelial cells) (Pajic-Lijakovic and Milivojevic, 2021). An increase in cell packing density $n_e > n_{conf}$ reduces the movement of epithelial cells from a convective to a conductive mechanism expressed as: $\vec{J}_e^{\,cond} = -D\vec{\nabla} n_e$ (where D is the mesoscopic diffusion coefficient of epithelial cells) (Pajic-Lijakovic and Milivojevic, 2021). The Marangoni flux of epithelial cells directs cell movement from the region of lower interfacial tension to that of higher interfacial tension and was expressed as: $\vec{J}_e^{\,m} = -k_{em} n_e \vec{\nabla}_s \gamma_{em}$ (where k_{em} is the mobility coefficient of epithelial cells coupling interfacial tension gradient to drift) (Pajic-Lijakovic et al., 2023b). The contact-mediated motility flux $\vec{J}_e^{\,cm}$ can be expressed in terms of a modified version of the model proposed by Armstrong et al. (2006) as: $\vec{J}_e^{\,cm} = \mu_e n_e \vec{\nabla} z_{em}$ (where μ_e is the motility coefficient of epithelial cells). Epithelial cells follow the gradient $\vec{\nabla} z_{em}$ by migrating from the region of higher coordination number z_{em} to that of lower coordination number. It is in accordance with the fact that epithelial cells avoid contact with mesenchymal cells. Heine et al. (2021) examined different breast co-culture systems and highlighted that the interactions at the biointerface between breast MCF-10A and MDA-MB-231 are the most dynamic in relation to neighboring exchanges. The epithelial-to-mesenchymal transition can be intensive along the biointerface (Barriga and Mayor, 2019). This phenomenon is accounted for through a sink term formulated here as: $S_{EMT} = -k_{EMT}(z_{em}) n_e$ (where $k_{EMT}(z_{em})$ is an increasing function of z_{em}).

The mass balance of mesenchymal cells can be expressed through a modified version of the model proposed by Pajic-Lijakovic et al. (2025b) as:

$$\frac{dn_m}{d\tau} + \vec{\nabla} \cdot \vec{J}_m = -S_{EMT} \quad (15)$$

where $\vec{J}_m$ is the flux of mesenchymal cells, which includes several contributions and can be expressed as: $\vec{J}_m = \vec{J}_m^{conv} + \vec{J}_m^{m} + \vec{J}_m^{CIL}$, $\vec{J}_m^{conv}$ is the convective flux, which is valid for a cell packing density $n_m \leq n_{conf}$ (Pajic-Lijakovic et al., 2025b), $\vec{J}_m^{m}$ is the Marangoni flux, and $\vec{J}_m^{cm}$ is the contact-mediated motility flux formulated here. The convective flux of mesenchymal cells can be expressed as: $\vec{J}_m^{conv} = -n_m \vec{v}_m$ (where $\vec{v}_m$ is the velocity of mesenchymal cells) (Pajic-Lijakovic et al., 2025b). The Marangoni flux of mesenchymal cells directs cell movement from the region of lower interfacial tension to that of higher interfacial tension and can be expressed as: $\vec{J}_m^{m} = -k_{Mm} n_m \vec{\nabla}_s \gamma_{em}$ (where k_{Mm} is the mobility coefficient of mesenchymal cells coupling interfacial tension gradient to drift) (Pajic-Lijakovic et al., 2023b). The contact-mediated motility flux $\vec{J}_m^{cm}$ directs movement of mesenchymal cells along the gradient of the coordination number z_{em} as: $\vec{J}_m^{cm} = \mu_m n_m \vec{\nabla} z_{em}$ (where μ_m is the motility coefficient of mesenchymal cells) (Armstrong et al., 2006). Consequently, mesenchymal cells migrate from regions of higher z_{em} to regions of lower z_{em}. The source term caused by the epithelial-to-mesenchymal transition S_{EMT} can be expressed as $S_{EMT} = k_{EMT}(z_{em}) n_e$.

In addition to the mass balance equations, it is also essential to establish the force balance equations for the subpopulations.

5.2 Force balances of the subpopulations

The main characteristic of migrating cell collectives is oscillations of the cell velocity, of the corresponding strain, and of the cell residual stress (Serra-Picamal et al., 2012; Notbohm et al., 2016; Pajic-Lijakovic et al., 2024b). The oscillatory change of cell velocity is an indicator of long-term inertial effects. The velocity of the epithelial subpopulation is equal to: $\vec{v}_e(\Re, \tau) = \frac{d\vec{u}_e}{d\tau}$, while that of the mesenchymal subpopulation is $\vec{v}_m(\Re, \tau) = \frac{d\vec{u}_m}{d\tau}$. The phenomenon has been discussed in the context of low-Reynolds turbulence, i.e., active turbulence, which represents a consequence of viscoelasticity in multicellular systems (Alert et al., 2022; Pajic-Lijakovic et al., 2024b). The inertial effects result from an imbalance between the driving and resistive forces. It is necessary to examine the contribution of each force in the dynamics at the biointerface, followed by formulation of the force balances for the subpopulations while considering inertial effects. The main characteristics of the forces are discussed in **Box 2**:

Box 2. The main characteristics of the forces that influence cell rearrangement of the subpopulations along the biointerface

Viscoelastic force (a resistive force) represents a consequence of the biointerface

stretching/compression caused by collective cell migration and can be expressed as: $\vec{\boldsymbol{F}}_{\boldsymbol{ve}}(\Re,\tau) = \nabla(\tilde{\boldsymbol{\sigma}}_{\boldsymbol{re}} - \tilde{\boldsymbol{\sigma}}_{\boldsymbol{rm}})$ (where $\tilde{\boldsymbol{\sigma}}_{\boldsymbol{re}}$ is the residual stress of epithelial subpopulation and $\tilde{\boldsymbol{\sigma}}_{\boldsymbol{rm}}$ is the residual stress of mesenchymal subpopulation along the biointerface defined in **Box 1**). This force decreases with an increase in the biointerface area as described in eq. 3. While mechanical stress and the viscoelastic force resist the migration of epithelial cells, they have no effect on the migration of mesenchymal cells. A compressive stress of 773 Pa restricts the mobility of epithelial cells, specifically MCF-10A and MCF-7, while simultaneously promoting the motility of mesenchymal cells, including 4T1, MDA-MB-231, and 67NR cells (Tse et al., 2012). Riehl et al. (2020) performed a study aimed at examining and contrasting the responses of mesenchymal MDA-MB-231 and MDA-MB-468 cells with those of epithelial MCF-10A cells when subjected to a shear stress of 1.5 Pa. Their results revealed that this specific level of shear stress promotes the mobility of MDA-MB-231 cells, does not influence MDA-MB-468 cells, and notably, diminishes the motility of MCF-10A epithelial cells.

Bending force (a resistive force) acts perpendicularly to the biointerface and can be expressed as: $\vec{\boldsymbol{F}}_{\boldsymbol{B}\,\boldsymbol{e}}(\Re,\tau) = n_e\vec{\boldsymbol{\nabla}}_{\perp}e_{eb}$ (where e_{eb} is the bending energy of the epithelial subpopulation along the biointerface and $\vec{\boldsymbol{\nabla}}_{\perp}$ is the normal gradient).

Marangoni force (a driving force) is tangential, tending to move both populations from the region of lower interfacial tension to that of higher interfacial tension along the biointerface. It is expressed as (Pajic-Lijakovic et al., 2023b): $\vec{\boldsymbol{F}}_{\boldsymbol{M}}(\Re,\tau) = \frac{1}{h}\vec{\boldsymbol{\nabla}}_{\boldsymbol{s}}\gamma_{em}$ (where h is the average size of a single cell). This force depends on the distance between the subpopulations d_{em}, and on the coordination number z_{em}. Repulsion between the subpopulations along the biointerface induces an increase in the interfacial tension.

Spreading force (a driving force) is correlated with the spreading factor, which governs wetting (extension)/de-wetting (compression) of the subpopulations. When the spreading factor is larger than zero, the subpopulation undergoes wetting, while otherwise, it undergoes de-wetting. Consequently, this force induces migration of the subpopulations perpendicular to the biointerface. The spreading force was expressed as (Pajic-Lijakovic et al., 2023b): $\vec{\boldsymbol{F}}_{\boldsymbol{Se}}(\Re,\tau) = n_eS^e\vec{\boldsymbol{u}}_{\boldsymbol{e}}$ for an epithelial subpopulation and $\vec{\boldsymbol{F}}_{\boldsymbol{Sm}}(\Re,\tau) = n_mS^m\vec{\boldsymbol{u}}_{\boldsymbol{m}}$ for a mesenchymal subpopulation (where S^e is the epithelial spreading factor: $S^e = \gamma_m - (\gamma_e + \gamma_{em})$ and S^m is the spreading factor of mesenchymal cells: $S^m = \gamma_e - (\gamma_m + \gamma_{em})$). When the interaction potential is attractive, i.e. $u_{int} < 0$ then the epithelial and mesenchymal subpopulations satisfy the conditions that: (i) $\gamma_e > \gamma_{em}$ and (ii) $\gamma_m \ll \gamma_e$ (Devanny et al., 2021; Pajic-Lijakovic et al., 2023b). Consequently, in this case, the epithelial subpopulation undergoes de-wetting ($S^e < 0$), while the mesenchymal subpopulation undergoes wetting ($S^m > 0$). The biointerface is then stable. However, when the interaction potential is repulsive than: (i) $\gamma_e < \gamma_{em}$ and (ii) $S^e < 0$ and $S^m < 0$. In this case, both subpopulations undergo de-wetting. The biointerface is then unstable (Pajic-Lijakovic et al., 2025b).

Friction force (a resistive force) depends on the relative velocity between the subpopulations along the biointerface $\vec{\boldsymbol{v}}_{\boldsymbol{R}} = \vec{\boldsymbol{v}}_{\boldsymbol{m}} - \vec{\boldsymbol{v}}_{\boldsymbol{e}}$ and the frictional coefficients for epithelial cells ξ_e and for mesenchymal cells ξ_m. (Pajic-Lijakovic et al., 2023b). This force for the epithelial subpopulation was expressed as: $\vec{\boldsymbol{F}}_{\boldsymbol{FR}}{}^{\boldsymbol{e}} = n_e\xi_e\vec{\boldsymbol{v}}_{\boldsymbol{R}}$ and for mesenchymal subpopulation is equal to: $\vec{\boldsymbol{F}}_{\boldsymbol{FR}}{}^{\boldsymbol{m}} = \boldsymbol{n_m}\xi_m\vec{\boldsymbol{v}}_{\boldsymbol{R}}$.

The force balance for the epithelial subpopulation can be expressed by modifying the force balance proposed by Pajic-Lijakovic et al. (2023b) as:

$$\langle m_e\rangle n_e\frac{D\vec{\boldsymbol{v}}_{\boldsymbol{e}}(\Re,\tau)}{D\tau} = \vec{\boldsymbol{F}}_{\boldsymbol{Se}} - \vec{\boldsymbol{F}}_{\boldsymbol{Be}} + \vec{\boldsymbol{F}}_{\boldsymbol{M}} - \vec{\boldsymbol{F}}_{\boldsymbol{ve}} - \vec{\boldsymbol{F}}_{\boldsymbol{FR}}{}^{\boldsymbol{e}} \quad (16)$$

where $\langle m_e \rangle$ is the average mass of a single epithelial cell and $\frac{D\vec{v}_e}{D\tau} = \frac{\partial \vec{v}_e}{\partial \tau} + (\vec{v}_e \cdot \vec{\nabla})\vec{v}_e$ is the material derivative (Bird et al., 1960). During the initial regime of segregation characterised by a larger biointerface, the force which predominantly reduces the movement of epithelial cells is friction caused by the shear stress generated along the biointerface, while the decreasing area of biointerface during the later regime of segregation increases the viscoelastic force. An increase in the compressive stress within the epithelial subpopulation and the associated increase in epithelial packing density intensify homotypic cell-cell interactions and, consequently, increase the contact inhibition of locomotion. The latter leads to weakening of cell-cell adhesion contacts and cell repolarisation, causing energy dissipation, which results in a decrease in the compressive stress so that cell migration can start again. The bending force is a resistive force that reduces biointerface bending during the segregation process. The spreading force primarily depends on the distance between the subpopulations d_{em} which influences the rate of epithelial de-wetting by increasing the interfacial tension. The Marangoni force depends on: (i) the distributions of the distance d_{em} and coordination number z_{em}, which affect the interaction potential and (ii) the curvature which influences epithelial surface tension.

The force balance for the mesenchymal subpopulation was expressed as (Pajic-Lijakovic et al., 2023b):

$$\langle m_m \rangle n_m \frac{D\vec{v}_m(\Re,\tau)}{D\tau} = \vec{F}_{Sm} + \vec{F}_M + \vec{F}_{ve} - \vec{F}_{FR}^{\,m} \quad (17)$$

where $\langle m_m \rangle$ is the average mass of a single mesenchymal cell and $\frac{D\vec{v}_m}{D\tau} = \frac{\partial \vec{v}_m}{\partial \tau} + (\vec{v}_m \cdot \vec{\nabla})\vec{v}_m$ is the material (total) derivative (Bird et al., 1960). In the case of mesenchymal cells, the frictional force reduces their movement. The viscoelastic force, which increases during the process of segregation, stimulates movement of mesenchymal cells. The spreading force drives wetting or de-wetting of the mesenchymal subpopulation depending on the distance d_{em}. The Marangoni force has a similar effect on both subpopulations by driving tangential movement of cells from the regions of lower interfacial tensions toward those of higher interfacial tension.

All these forces change the velocities and strains of the subpopulations, as well as the area of the biointerface. These changes influence mechanical stresses within the subpopulations accompanied by the interfacial tension. Consequently, this cause-consequence cycle has a feedback impact on the volumetric and dilational viscoelasticity of these co-cultured multicellular systems and on the efficiency of spreading the cancer mesenchymal-like subpopulation in the presence of epithelial cells. The segregation process attains equilibrium when the driving forces and resistive forces are balanced.

6. Interrelationship between physical parameters involved in mechanical coupling between the subpopulations

The segregation of subpopulations via collective cell migration within co-cultured spheroids generates macroscopic mechanical stress. This stress depends on the mechanical stress within the subpopulations and the stress generated along the biointerface due to heterotypic cell-cell interactions. The efficiency of the segregation process, accompanied by spreading of cancer mesenchymal-like cells through the epithelium, depends on the distribution of macroscopic stress and the volume fraction of the epithelial

subpopulation quantified by the divergence of the macroscopic stress and gradient of the volume fraction of epithelial cells. Contact dynamics along the biointerface, through the interfacial tension, influences the distribution of macroscopic stress: (i) directly by influencing the stress along the biointerface and the stress within the subpopulations and (ii) indirectly by influencing the mechanical coupling between the subpopulations by changing the area of the biointerface. A larger area of biointerface ensures intensive energy transfer and dissipation along the biointerface, leading to a more homogeneous distribution of macroscopic stress. Correspondingly, a decrease of biointerface area during the segregation process results in increased inhomogeneity of the macroscopic stress, which has the potential to speed up the segregation process and the spreading of cancer. When epithelial cells reach into the core region, while cancer cells are grouped within the surface region of the spheroid, the biointerface area and the average coordination number are minimal, i.e., A_{min} and $\langle z_{em} \rangle^{min}$. In this case, the stress difference between the subpopulations is maximal $(\tilde{\boldsymbol{\sigma}}_{\boldsymbol{re}} - \tilde{\boldsymbol{\sigma}}_{\boldsymbol{rm}})_{max}$. This state of the spheroid corresponds to complete segregation achieved under static equilibrium between the driving and resistive forces. The relationships between the physical parameters on various space scales are shown in **Figure 3**:

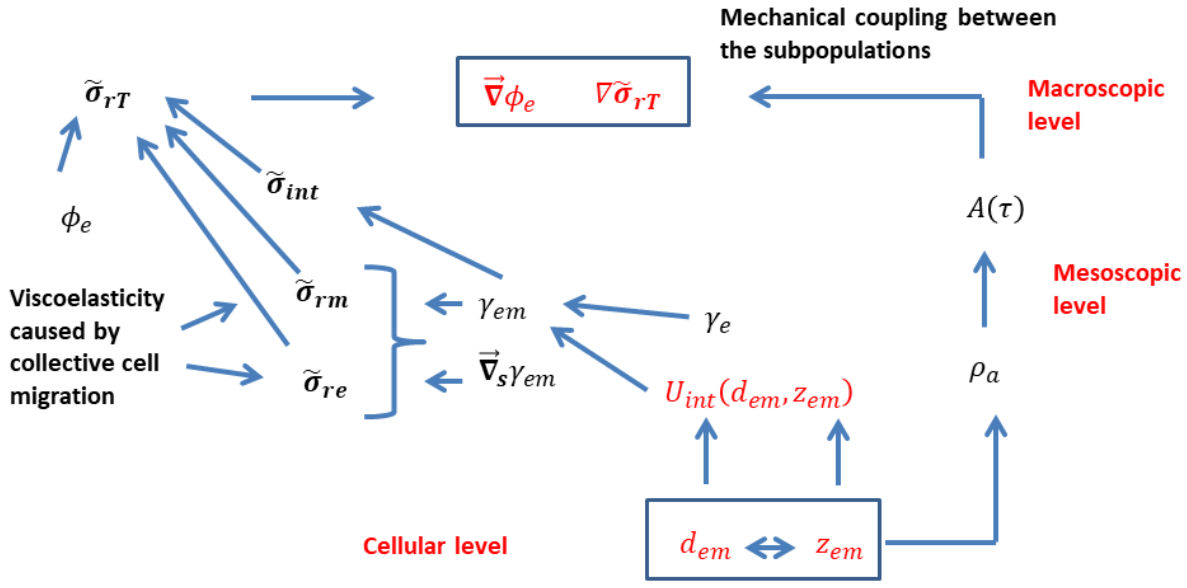

Figure 3. The relationships between physical parameters on various space scales which influence the segregation process and the efficiency of cancer spreading through epithelium.

Stresses within the subpopulations are influenced not only by interfacial tension and the gradient of interfacial tension, but also by viscoelasticity caused by collective cell migration. Interfacial tension, as the one of the main factors responsible for the dynamics along the biointerface, depends on the epithelial surface tension and interaction potential. The epithelial surface tension, as a measure of epithelial cohesion, relies on the biointerface bending and has the potential to minimize the in-plane surface energy. The viscoelastic nature of epithelial surfaces was discussed in the context of the proposed $\gamma_e - \frac{\Delta A}{A}$ constitutive model of dilational viscoelasticity, based on various experimental findings on *in vitro* model systems.

Contact dynamics between the subpopulations can be characterized by the coordination number z_{em} and distance between the subpopulations d_{em} on a cellular level. Both parameters influence the interaction potential, while the distribution of the coordination number influences the area of the biointerface.

A few controlling dimensionless numbers can be identified such as: (i) the dimensionless interfacial tension $\frac{\gamma_{em}}{\gamma_e}$ (from eq. 10), (ii) the fraction of interfacial stress in the total macroscopic stress $\frac{\tilde{\sigma}_{int}}{\tilde{\sigma}_{rT}}$ (from eq. 1), and (iii) the dimensionless viscoelasticity number equal to $\frac{G'(r,\omega)}{G''(r,\omega)}$ (where $G'(r,\omega)$ is the storage modulus, $G''(r,\omega)$ is the loss modulus, ω is the angular velocity equal to $\omega = \frac{2\pi}{T}$, and T is the period of oscillation of the biointerface caused by wetting/de-wetting of the subpopulation and corresponds to a few hours). Storage and loss moduli can be extracted from the proposed constitutive models described in **Box 1**, which are presented in the **Appendix**. When $\frac{\gamma_{em}}{\gamma_e} < 1$, attractive interactions dominate along the bioinerface and the biointerface is stable. However, when $\frac{\gamma_{em}}{\gamma_e} > 1$, repulsive interactions dominate and the biointerface is unstable. The fraction of interfacial stress in the total macroscopic stress quantifies the impact of mechanical stress generated along the biointerface in the total macroscopic stress which has a feedback impact on the efficiency of the segregation process. The dimensionless viscoelasticity number $\frac{G'(r,\omega)}{G''(r,\omega)}$ can be correlated with the mobility of the subpopulations. Higher values of $\frac{G'(r,\omega)}{G''(r,\omega)}$ point to a subpopulation that is less mobile.

7. **Outlook: experimental tests**

To gain a more profound understanding of the dynamics at the biointerface, which is essential for preventing the invasion of the epithelium by cancer cells, further experiments are required to determine a few physical parameters such as: (i) the coordination number z_{em} distribution, (ii) the epithelial surface tension γ_e, (iii) the epithelial-mesenchymal interfacial tension γ_{em}, and (iv) the residual stresses generated within the subpopulations. The coordination number distributions can be quantified from 3D imaging by combining confocal or light-sheet microscopy with automated cell segmentation using nucleus- or membrane-based approaches. Cell–cell contacts are identified by shared interfacial area or short-distance criteria between segmented cell surfaces, allowing heterotypic neighbors to be

distinguished based on cell-type labeling. For each epithelial cell at the biointerface, the coordination number is defined as the number of adjacent mesenchymal cells, yielding spatially resolved distributions that can be correlated with interface curvature or mechanical readouts (Stringer et al., 2021; Gómez et al., 2021). The epithelial/mesenchymal coordination number can be correlated with epithelial surface tension and epithelial-mesenchymal interfacial tension.

Although the surface tension of multicellular systems is known to vary with time and space (i.e., dynamic surface tension), there are currently no empirical data supporting the notion of temporal fluctuations in this physical property. Thus far, only a static (equilibrium) value for surface tension has been observed and measured as a characteristic of external multicellular surfaces in contact with liquid medium. A range of methods has been employed, including: uni-axial compression of mono-cultured spheroids positioned between parallel plates (Mombach et al., 2005), micropipette aspiration of spheroids (Guevorkian et al., 2021), and the use of a magnetic tensiometer (Nagle et al., 2022). The existing literature indicates that the static surface tension observed in multicellular systems is influenced not only by the type of cells present but also by the measurement techniques employed. Magnetic field can enhance the strength of these cell-cell adhesion contacts and on that basis lead to an increase in the surface tension (Jafari et al., 2019).

The dynamic interfacial tension between epithelial and mesenchymal subpopulations has yet to be investigated experimentally. Resonant acoustic rheometry presents a feasible approach for quantifying this phenomenon. This method has proven effective in measuring surface and interfacial tensions within soft matter systems, including hydrogels (Hobson et al., 2021).

Determining the 3D stress distribution is a considerable challenge. To tackle this difficulty, numerous studies have introduced inclusions in the form of microbead or droplet-based stress sensors, which have well-defined mechanical properties, into 3D cellular systems to mitigate the complexities associated with 3D traction force microscopy (Zhang et al., 2017). Incompressible micro-droplet sensors can be utilized to assess the anisotropic normal stress component (Campàs et al., 2013). Dolega et al. (2017) developed elastic microbead sensors to quantify the isotropic compressive stress resulting from tumor growth within the matrix (i.e., solid stress). These inclusion-based experimental techniques allow for the measurement of stress values in close proximity to the inclusion.

8. Conclusion

The formation of sharp biointerfaces between different cell subpopulations is crucial for the preservation of tissue organization and homeostasis. Alterations of the biointerface between epithelial and cancer cells provides an indicator of cancer development. Gaining deeper insight into the dynamics at the biointerface is a first step in identifying strategies to prevent cancer dissemination. The role of the dynamics along the biointerface in the spreading of cancer cells was discussed on the basis of simple model systems such as the segregation of epithelial and cancer mesenchymal-like subpopulations within co-cultured spheroids via collective cell migration.

The importance of mechanical forces in tissue self-organisation and the spreading of cancer was first recognized more than two decades ago. We have tried to extend this research by pointing to: (i) contact dynamics along the epithelial-mesenchymal biointerface and its influence on the segregation process and (ii) the volumetric viscoelasticity of the subpopulations and the dilational viscoelasticity of the biointerface. In the present paper we have discussed mechanical coupling between the subpopulations based on: (i) interrelationship between macroscopic stress within part of the spheroid and the size of the biointerface on the macroscopic scale, (ii) postulated mass and force balances of the subpopulations along the biointerface on the mesoscopic scale, and (iii) the interaction potential, which has a feedback impact on the interfacial tension on the cellular scale. The main results were obtained by combining multi-scale models with the results of biological and bio-mechanical experiments, and we can summarize them as follows:

- Higher divergence of macroscopic stress, induced by a decrease in size of the biointerface area, ensures efficient segregation of the subpopulations and cancer spreading through epithelium.
- Decrease of the biointerface area is affected by the interfacial tension.
- The divergence of macroscopic stress depends on the variations of: (i) the interfacial tension along the biointerface and (ii) mechanical stress within the subpopulations.
- Mechanical stress stimulates movement of cancer cells.
- Higher interfacial tension ensures efficient segregation of the subpopulations and spreading of cancer. Repulsive heterotypic cell-cell interactions, significant at shorter distances between the subpopulations, increase the interfacial tension.

The multi-scale biophysics model introduced in this review represents merely an initial phase in the modeling of intricate multi-cellular spheroids. Further experiments are required to quantify the interfacial tension between the subpopulations, as well as the gradient of this tension, and to relate them to the accumulation of residual stress in cells. The collection of experimental data necessary to parameterize such multi-scale and multi-phase models will constitute another crucial step in the modeling process.

Conflict of interest: The authors report there is no conflict of interest.

Funding: This work was supported in part by the Engineering and Physical Sciences Research Council, United Kingdom (grant number EP/X004597/1) and by the Ministry of Science, Technological Development and Innovation of the Republic of Serbia (Contract No. 451-03-136/2025-03/200135).

Appendix

Proposed constitutive models for epithelial and mesenchymal subpopulations discussed in **Box 1** and storage and loss moduli obtained from these models by Fourier transform is presented in **Table 2**:

Table 2. Constitutive models for epithelial and mesenchymal subpopulations and corresponding storage and loss moduli

model	Model equation	Storage modulus	Loss modulus
Cancer-mesenchymal subpopulation Maxwell model	$\tilde{\boldsymbol{\sigma}}_{\boldsymbol{m}} + \tau_R \dot{\tilde{\boldsymbol{\sigma}}}_{\boldsymbol{m}} = \eta_m \dot{\tilde{\boldsymbol{\varepsilon}}}_{\boldsymbol{m}}$	$\frac{\eta_m \tau_R \omega^2}{1+\tau_R^2\omega^2}$	$\frac{\eta_m \omega}{1+\tau_R^2\omega^2}$
Epithelial subpopulation Zener model	$\tilde{\boldsymbol{\sigma}}_{\boldsymbol{e}} + \tau_R \dot{\tilde{\boldsymbol{\sigma}}}_{\boldsymbol{e}} = E_e \tilde{\boldsymbol{\varepsilon}}_{\boldsymbol{e}} + \eta_e \dot{\tilde{\boldsymbol{\varepsilon}}}_{\boldsymbol{e}}$	$\frac{E_e + \eta_e \tau_R \omega^2}{1+\tau_R^2\omega^2}$	$\frac{\eta_e \omega - E_e \tau_R \omega}{1+\tau_R^2\omega^2}$
Epithelial subpopulation Kelvin-Voigt model	$\tilde{\boldsymbol{\sigma}}_{\boldsymbol{e}} = E_e \tilde{\boldsymbol{\varepsilon}}_{\boldsymbol{e}} + \eta_e \dot{\tilde{\boldsymbol{\varepsilon}}}_{\boldsymbol{e}}$	η_e	$\eta_e \omega$
Epithelial subpopulation Fractional model	$\tilde{\boldsymbol{\sigma}}_{\boldsymbol{e}} = \eta_\alpha D^\alpha(\tilde{\boldsymbol{\varepsilon}}_{\boldsymbol{e}})$	$\eta_\alpha \omega^\alpha cos\left(\frac{\pi\alpha}{2}\right)$	$\eta_\alpha \omega^\alpha sin\left(\frac{\pi\alpha}{2}\right)$

where $\eta_m(r)$ and $\eta_e(r)$ are the viscosities of the mesenchymal and epithelial subpopulations, respectively, $E_e(r)$ is the elastic modulus of the epithelial subpopulation, τ_R is the stress relaxation time, $\tilde{\boldsymbol{\sigma}}_{\boldsymbol{e}}$ **and** $\tilde{\boldsymbol{\sigma}}_{\boldsymbol{m}}$ are stresses within the mesenchymal and epithelial subpopulations, $\tilde{\boldsymbol{\varepsilon}}_{\boldsymbol{e}}$ is the epithelial strain, $\dot{\tilde{\boldsymbol{\varepsilon}}}_{\boldsymbol{m}}$ and $\dot{\tilde{\boldsymbol{\varepsilon}}}_{\boldsymbol{e}}$ are mesenchymal and epithelial strain rates caused by collective cell migration, $\dot{\tilde{\boldsymbol{\sigma}}}_{\boldsymbol{m}}$ **and** $\dot{\tilde{\boldsymbol{\sigma}}}_{\boldsymbol{e}}$ are rates of change of the mesenchymal and epithelial stresses, $\eta_\alpha(r)$ is the effective modulus, and $D^\alpha(\tilde{\boldsymbol{\varepsilon}}_{\boldsymbol{e}})$ is the fractional derivative, and α is the order of the fractional derivative. Caputo's definition of the fractional derivative of a function $\tilde{\boldsymbol{\varepsilon}}(r,\tau)$ was used, and it is given as: $D^\alpha \tilde{\boldsymbol{\varepsilon}} = \frac{1}{\Gamma(1-\alpha)} \frac{d}{d\tau} \int_0^\tau \frac{\tilde{\varepsilon}(r,\tau')}{(\tau-\tau')^\alpha} d\tau'$ (where $\Gamma(1-\alpha)$ is a gamma function) (Podlubny, 1999).

References

1. Alert, R. and Trepat, X. 2020) Physical models of collective cell migration. Ann. Rev. Cond. Matter Phys. 11:77-101, doi.org/10.1146/annurev-conmatphys-031218-013516.
2. Alert, R., Casademunt, J., J-F. Joanny. 2022. Active turbulence. Annu. Rev. Condens. Matter Phys. 13, 143–70, https://doi.org/10.1146/annurev-conmatphys-082321-035957.
3. Alt, S., Ganguly, P., Salbreux, G. 2017. Vertex models: from cell mechanics to tissue morphogenesis. Philosoph. Trans. Roy. Soc. B: Biol. Sci. 372(1720), 20150520, https://doi.org/10.1098/rstb.2015.0520.
4. Angelini, T.E., Hannezo, E., Trepat, X., Marquez, M., Fredberg, J.J., Weitz, D.A. 2011. Glass-like dynamics of collective cell migration. PNAS 108(12), 4714–4719, https://doi.org/10.1073/pnas.1010059108
5. Armstrong, N.J., Painter, K.J., Sherratt, J.A. 2006. A continuum approach to modelling cell–cell adhesion. J. Theor. Biol. 243, 98–113, https://doi.org/10.1016/j.jtbi.2006.05.030.
6. Audoly, B. and Pomeau, Y. 2010. Elasticity and Geometry: From Hair Curls to the Non-linear Response of Shells. Oxford University Press Inc., New York pp. 192.
7. Barriga, E.H. and Mayor, R. 2019. Adjustable viscoelasticity allows for efficient collective cell migration. Sem. Cell Dev. Biol. 93, 55-68, https://doi.org/10.1016/j.semcdb.2018.05.027.
8. Barriga, E.H., Franze, K., Charras, G., Mayor R. 2018. Tissue stiffening coordinates morphogenesis by triggering collective cell migration in vivo. Nature 554(7693), 523–527, doi:10.1038/nature25742.
9. Batlle, E. and Wilkinson, D.G. 2012. Molecular Mechanisms of Cell Segregation and Boundary Formation in Development and Tumorigenesis. Cold Spring Harb. Persp. Biol. 4:a008227, doi: 10.1101/cshperspect.a008227.
10. Beaune, G., Blanch-Mercader, C., Douezan, S., Dumond, J., Gonzalez-Rodriguez, D., Cuvelier, D., Ondarçuhu, T., Sens, P., Dufour, S., Murrell, M.P., Brochard-Wyarta, F. 2018. Spontaneous migration of cellular aggregates from giant keratocytes to running spheroids. PNAS 115 (51), 12926-12931, DOI: 10.1073/pnas.1811348115.
11. Blanchard, G.B., Fletcher, A.G., Schumacher, LJ. 2019. The devil is in the mesoscale: mechanical and behavioural heterogeneity in collective cell movement. Sem. Cell Dev. Biol. 93, 46-54, doi.org/10.1016/j.semcdb.2018.06.003.
12. Binysh, J., Wilks, T.R., Souslov, A. 2022. Active elastocapillarity in soft solids with negative surface tension. Sci. Adv. 8, eabk3079, DOI: 10.1126/sciadv.abk307.
13. Bird, R.B., Stewart, W.E., Lightfoot, E.N. 1960. Transport Phenomena. New York, London, John Wiley & Sons INC p. 84.
14. Brayford, S., Kenny, F.N., Hiratsuka, T., Serna-Morales, E., Yolland, L., Luchici, A., Stramer, B.M. 2019. Heterotypic contact inhibition of locomotion can drive cell sorting between epithelial and mesenchymal cell populations. J. Cell Sci 132(11), jcs223974. https://doi.org/10.1242/jcs.223974.

15. Campàs, O., Mammoto, T., Hasso, S., Sperling, R.A., O'Connell, D., Bischof, A.G., Maas, R., Weitz, D.A,, Mahadevan, L., Ingber, D.E. 2013. Quantifying cell-generated mechanical forces within living embryonic tissues. Nature Meth. 11(2):183-189, doi:10.1038/nmMeth.2761.
16. Campbell, K., Rossi, F., Adams, J., Pitsidianaki, I., Barriga, F.M., Garcia-Gerique, L., Batlle, E., Casanova, J., Casali, A. 2019. Collective cell migration and metastases induced by an epithelial-to-mesenchymal transition in Drosophila intestinal tumours. Nature Comm. 10, 2311, DOI: 10.1038/s41467-019-10269-y.
17. Carey, S.P., Starchenko, A., McGregor, A.L., Reinhart-King, C.A. 2013. Leading malignant cells initiate collective epithelial cell invasion in a three-dimensional heterotypic tumor spheroid model. Clin Exp Metast 30, 615–630, DOI 10.1007/s10585-013-9565-x.
18. Cieślik, M., Hoang, S.A., Baranova, N., Chodaparambil, S., Kumar, M., Allison, D.F., Xu, X., Wamsley, J., Gray, L., Jones, D.R., Mayo, M.W., Bekiranov, S. 2013. Epigenetic coordination of signaling pathways during the epithelial-mesenchymal transition. Epigen. Chrom. 6, 28, doi: 10.1186/1756-8935-6-28.
19. Coburn, L., Cerone, L., Torney, C., Couzin, I.D., Neufeld, Z. 2013. Tactile interactions lead to coherent motion and enhanced chemotaxis of migrating cells. Phys. Biol. 10(4), 046002., https://doi.org/10.1088/1478-3975/10/4/046002.
20. Deforet, M., Hakim, V., Yevick, H., Duclos, G., Silberzan, P. 2014. Nature Comm. 5(1), 3747, https://doi.org/10.1038/ncomms4747.
21. Devanny, A.J., Vancura, M.B., Kaufman, L.J. 2021. Exploiting differential effects of actomyosin contractility to control cell sorting among breast cancer cells. Mol. Biol. Cell 32, ar24, doi.org/10.1091/mbc.E21-07-0357.
22. Dolega, M.E., Delarue, M., Ingremeau, F., Prost, J., Delon, A., Cappello, G. 2017. Cell-like pressure sensors reveal increase of mechanical stress towards the core of multicellular spheroids under compression, Nature Comm. 8, 14056 1-9, DOI: 10.1038/ncomms14056.
23. Fletcher, A.G., Osterfield, M., Baker, R.E., Shvartsman, S.Y. 2014. Vertex models of epithelial morphogenesis. Biophys. J. 106(11), 2291–2304, https://doi.org/10.1016/j.bpj.2013.11.4498.
24. Friedl, P., and Gilmour, D. 2009. Collective cell migration in morphogenesis, regeneration and cancer. Nature Rev. Mol. Cell Biol. 10(7), 445–457. https://doi.org/10.1038/nrm2720
25. Graner, F., and Glazier, J. A. 1992. Simulation of biological cell sorting using a two-dimensional extended Potts model. Phys. Rev. Let, 69(13), 2013–2016., https://doi.org/10.1103/PhysRevLett.69.2013.
26. Gómez, H. F., Dumond, M. S., Hodel, L., Vetter, R., Iber, D. 2021. 3D cell neighbour dynamics in growing pseudostratified epithelia. eLife, 10, e68135. https://doi.org/10.7554/eLife.68135.
27. Grosser, S., Lippoldt, J., Oswald, L., Merkel, M., Sussman, D.M., Renner, F, Gottheil, P., Morawetz, E.W., Fuhs, T., Xie, X. et al. 2021. Cell and Nucleus Shape as an Indicator of Tissue Fluidity in Carcinoma. Phys. Rev. X 11, 011033, DOI: 10.1103/PhysRevX.11.011033.
28. Gsell, S., Tlili, S., Merkel, M., Lenne, P-F. 2023. Marangoni-like tissue flows enhance symmetry breaking of embryonic organoids. bioRxiv doi.org/10.1101/2023.09.22.559003.
29. Guan, L-Y., Lin S-Z., Chen, P-C., Lv J-Q., Li, B., Feng, X-Q. 2023. Interfacial organization and forces arising from epithelial−cancerous monolayer interactions. Asc Nano 17(24), 24668-24684, doi: 10.1021/acsnano.3c03990.

30. Guevorkian, K., Brochard-Wyart, F., Gonzalez-Rodriguez, D. 2021. Flow dynamics of 3D multicellular systems into capillaries, in Viscoelasticity and collective cell migration, eds. Pajic-Lijakovic I, Barriga E (Academic Press, US), p. 193.
31. Hauseux, P., Ambrosetti, A., Bordas, S. P. A., Tkatchenko, A. 2022. Colossal enhancement of atomic force response in van der Waals materials arising from many-body electronic correlations. Phys. Rev. Lett. 128(10), 106101, https://doi.org/10.1103/PhysRevLett.128.106101.
32. Heine, P., Lippoldt, J., Reddy, G.A., Katira, P., Kaes, J. 2021. Anomalous cell sorting behaviour in mixed monolayers discloses hidden system complexities. New J. Phys. 23, 043034, https://doi.org/10.1088/1367-2630/abf273.
33. Hingangavkar, G.M. 2025. Applied Mathematical and Computational Frameworks in Materials Science: A Comprehensive Review. Next Research, in press. https://doi.org/10.1016/j.nexres.2025.101224.
34. Hobson, E. C., Li, W., Juliar, B.A., Putnam, A.J., Stegemann, J.P., Deng, C.X. 2021. Resonant acoustic rheometry for non-contact characterization of viscoelastic biomaterials. Biomaterials, 269, 120676. https://doi.org/10.1016/j.biomaterials.2021.120676.
35. Huang, Y.L., Shiau, C., Wu, C., Segall, J.E., Wu, M. 2020. The architecture of co-culture spheroids regulates tumor invasion within a 3D extracellular matrix. Biophys. Rev. Lett. 15(3), 131–141, doi:10.1142/s1793048020500034.
36. Kabla, A.J. 2012. Collective cell migration: leadership, invasion and segregation. Nature Phys. 8(4), 262–271., https://doi.org/10.1038/nphys2259.
37. Kachalo, S., Naveed, H., Cao, Y., Zhao, J., Liang, J. 2015. Mechanical Model of Geometric Cell and Topological Algorithm for Cell Dynamics from Single-Cell to Formation of Monolayered Tissues with Pattern. PLoS ONE 10(5), e0126484. doi:10.1371/journal.pone.0126484.
38. Le, H.A. and Mayor, R. 2023. Cell–matrix and cell–cell interaction mechanics in guiding migration. Biochem. Soc. Trans. doi.org/10.1042/BST20230211.
39. Lucia, S.E., Jeong, H., Shin, J.H. 2022. Cell segregation via differential collision modes between heterotypic cell populations. Mol. Biol. Cell 33, ar129, 1–12, doi.org/10.1091/mbc.E22-03-0097.
40. Israelachvili, J.N. 2011. Intermolecular and Surface Forces (3rd ed.). Academic Press.
41. Jafari, J., Han, X-I., Palmer, J., Tran, P.A., O'Connor, A.J. 2019. Remote Control in Formation of 3D Multicellular Assemblies Using Magnetic Forces. ASC Biomat. Sci. Eng. 5, 2532-2542, DOI: 10.1021/acsbiomaterials.9b00297.
42. Kang, W., Ferruzzi, J., Spatarelu, C-P., Han, Y.L., Sharma, Y., Koehler, S.A., Mitchel, J.A., Khan, A., Butler, J.P., Roblyer, D., Zaman, M.H., et al. 2021. A novel jamming phase diagram links tumor invasion to non-equilibrium phase separation iSci. 24, 103252, DOI: 10.1016/j.isci.2021.103252.
43. Karbalaei, A., Kumar, R., Cho, H.J. 2016. Thermocapillarity in Microfluidics—A Review. Micromachines 7, 13, doi:10.3390/mi7010013.
44. Kenny, P.A., Lee, G.Y., Myers, C.A., Neve, R.M., Semeiks, J.R., Spellman, P.T., Lorenz, K., Lee, E.H., Barcellos-Hoff, M.H., Petersen, O.W., et al. 2007. The morphologies of breast cancer cell lines in three-dimensional assays correlate with their profiles of gene expression. Mol. Oncol. 1, 84-96, doi:10.1016/j.molonc.2007.02.004.

45. Kezwon, A. and Wojciechowski, K. 2014. Effect of temperature on surface tension and surface dilational rheology of type I collagen. Coll. Surf. A: Phys. Eng. Aspects 460, 168-175, doi.org/10.1016/j.colsurfa.2014.05.025.
46. Khalilgharibi, N., Fouchard, J., Asadipour, N., Yonis, A., Harris, A., Mosaff, P., Fujita, Y., Kabla, A., Baum, B., Muñoz, J.J., Miodownik, M., Charras, G. 2019. Stress relaxation in epithelial monolayers is controlled by actomyosin. Nat. Phys. 15, 839-847, DOI: 10.1038/s41567-019-0516-6.
47. Lee, P. and Wolgemuth, C.W. 2011. Wounds without Purse tiring or signaling. PLoS Comp. Biol. 7(3), e1002007 1-8, DOI: 10.1371/journal.pcbi.1002007.
48. Li, Y., Naveed, H., Liang, J., Xu, L.X. 2014. Effects of Mechanical Properties on Tumor Invasion: Insights from a Cellular Model. Annual International Conference of the IEEE Engineering in Medicine and Biology Society. IEEE Engineering in Medicine and Biology Society 6818-6821.
49. Marmottant, P., Mgharbel, A., Kafer, J., Audren, B., Rieu, J.P., Vial, J.C., van der Sanden, B., Maree, A.F.M., Graner, F., Delanoe-Ayari, H. 2009. The role of fluctuations and stress on the effective viscosity of cell aggregates. PNAS 106(41), 17271-17275, doi.org/10.1073/pnas.090208510.
50. Méhes, E., Mones, E., Varga, M., Zsigmond, Á., Biri-Kovács, B., Nyitray, L., Barone, V., Krens, G., Heisenberg, C-P., Vicsek, T. 2023. 3D cell segregation geometry and dynamics are governed by tissue surface tension regulation. Comm. Biol. 6, 817. https://doi.org/10.1038/s42003-023-05181-7.
51. Mierke, C.T. 2019. The role of the optical stretcher in investigating cell mechanics regulating cell adhesion and motility. Front. Cell Dev. Biol., 7, 184, https://doi.org/10.3389/fcell.2019.00184.
52. Mierke, C.T. 2024. Extracellular matrix cues regulate mechanosensing and mechanotransduction of cancer cells. Cells, 13(1), 96. https://doi.org/10.3390/cells13010096.
53. Millar, F.R., Janes, S.M., Giangreco, A. 2017. Epithelial cell migration as a potential therapeutic target in early lung cancer. Europ. Resp. Rev. 26, 160069, DOI: 10.1183/16000617.0069-2016.
54. Mombach, J.C.M., Robert, D., Graner, F., Gillet, G., Thomas, G.L., Idiart, M., Rieu, J.P. 2005. Rounding of aggregates of biological cells: Experiments and simulations. Phys. A 352:525-534, doi:10.1016/j.physa.2005.02.008.
55. Nagle, I., Richert, A., Quinteros, M., Janel, S., Buysschaert, E., Luciani, N., Debost, H., Thevenet, V., Wilhelm, C., Prunier, C., Lafont, F., Padilla-Benavides, T., Boissan, M., Reffay, M. 2022. Surface tension of model tissues during malignant transformation and epithelial–mesenchymal transition. Front. Cell Dev. Biol. DOI 10.3389/fcell.2022.926322.
56. Niculescu, I., Textor, J., and de Boer, R. J. 2015. Crawling and gliding: a computational model for shape-driven motility of eukaryotic cells. PLOS Computational Biology, 11(10), e1004280, https://doi.org/10.1371/journal.pcbi.1004280.
57. Nikkhah, M., Strobl, J.S., Schmelz, E.M., Roberts, P.C., Zhou, H., Agah, M. 2011. MCF10A and MDA-MB-231 human breast basal epithelial cell co-culture in silicon micro-arrays. Biomaterials 32, 7625-7632, DOI: 10.1016/j.biomaterials.2011.06.041.
58. Nnetu, K.D., Knorr, M., Pawlizak, S., Fuhs, T., Kaes, J. 2013. Slow and anomalous dynamics of an MCF-10A epithelial cell monolayer. Soft matter 9, 9335-9341, https://doi.org/10.1039/C3SM50806D.

59. Notbohm, J., Banerjee, S., Utuje, K.J.C., Gweon, B., Jang, H., Park, Y., Shin, J., Butler, J.P., Fredberg, J.J., Marchetti, M.C. 2016. Cellular contraction and polarization drive collective cellular motion. Biophys. J. 110, 2729-2738, DOI: 10.1016/j.bpj.2016.05.019.
60. Pajic-Lijakovic, I. and Milivojevic, M. 2025a. Entropy Production in Epithelial Monolayers Due to Collective Cell Migration. Entropy 27(5), 483, DOI: 10.3390/e27050483.
61. Pajic-Lijakovic, I., Milivojevic, M., McClintock, P.V.E. 2025b. The role of epithelial-mesenchymal interfacial tension in biological systems. Front. Phys. 20(4), 044300, DOI: 10.15302/frontphys.2025.044300.
62. Pajic-Lijakovic, I., Eftimie, R., Milivojevic, M., Bordas, S.P.A. 2024a. Segregation of co-cultured multicellular systems: review and some modeling consideration. Quart. Rev. Biophys. 57(e5), 1-17, DOI: 10.1017/S0033583524000015
63. Pajic-Lijakovic, I., Milivojevic, M., McClintock, P.V.E. 2024b. Role of viscoelasticity in the appearance of low-Reynolds turbulence: Considerations for modelling. J. Biol. Eng. 18, 24, https://doi.org/10.1186/s13036-024-00415-6.
64. Pajic-Lijakovic, I., Eftimie, R., Milivojevic, M., Bordas, S.P.A. 2023a. Multi-scale nature of the tissue surface tension: theoretical consideration on tissue model systems. Adv. Colloid Interface Sci. 315, 102902, DOI: 10.1016/j.cis.2023.102902.
65. Pajic-Lijakovic, I. and Milivojevic, M. 2023b. Dynamics along the epithelial-cancer biointerface: hidden system complexities. Biocell 47(11), 2321-2334, DOI: 10.32604/biocell.2023.043796.
66. Pajic-Lijakovic, I. and Milivojevic, M. 2023c. Morphological changes of epithelial cells and spreading of cancer: theoretical consideration. Appl. Phys. A 129, 553, DOI: 10.1007/s00339-023-06814-8.
67. Pajic-Lijakovic, I. and Milivojevic, M. 2021. Viscoelasticity and cell jamming state transition. Europ Phys J Plus 136, 750, DOI: 10.1101/2021.03.19.436195.
68. Petrolli V, Boudou T, Balland M, Cappello G. Oscillations in collective cell migration, in Viscoelasticity and Collective Cell Migration: An Interdisciplinary Perspective Across Levels of Organization, eds. by I. Pajic-Lijakovic, E. Barriga (Academic Press, US, 2021), p. 157.
69. Petrungaro, G., Morelli, L., Uriu, K. 2019. Information flow in the presence of cell mixing and signaling delays during embryonic development. Sem. Cell Dev. Biol. 93, 26-35, DOI: 10.1016/j.semcdb.2018.09.008.
70. Pitenis, A.A., Urueña, J.M., Hart, S.M., O'Bryan, C.S., Marshall, S.L., Levings, P.P., Angelini, T.E., Sawyer, W.G. 2018. Friction-Induced Inflammation. Tribol. Lett. 66-81, doi.org/10.1007/s11249-018-1029-7.
71. Podlubny, I. 1999. Fractional Differential Equations, Mathematics in Science and Engineering. London Academic Press, 198, pp. 78.
72. Pollard, T.D. and Borisy, G.G. 2003. Cellular motility driven by assembly and disassembly of actin filaments. Cell, 112, 453–465, DOI: 10.1016/s0092-8674(03)00120-x.
73. Riehl, B.D., Kim, E., Lee, J.S., Duan, B., Yang, R., Donahue, H.J., Lim, J.Y. 2020. The Role of Fluid Shear and Metastatic Potential in Breast Cancer Cell Migration. J. Biomech. Eng. 142, 101001 doi: 10.1115/1.4047076.

74. Riehl, B.D., Kim, E., Bouzid, T., Lim, Y.J. 2021. The Role of Microenvironmental Cues and Mechanical Loading Milieus in Breast Cancer Cell Progression and Metastasis. Front. Bioeng. Biotechnol. 8, 608526, DOI: 10.3389/fbioe.2020.608526.
75. Roycroft, A. and Mayor, R. 2016. Molecular basis of contact inhibition of locomotion. Cell. Mol. Life Sci. 73, 1119–1130, DOI: 10.1007/s00018-015-2090-0.
76. Shen, Z., Sosa, R. I., Lengiewicz, J., Tkatchenko, A., Bordas, S.P.A. 2025. Machine learning surrogate models of many-body dispersion interactions in polymer melts. arXiv:2503.15149. https://doi.org/10.48550/arXiv.2503.15149.
77. Senigagliesi, B., Samperi, G., Cefarin, N., Gneo, L., Petrosino, S., Apollonio, M., Caponnetto, F., Sgarra, R., Collavin, L., Cesselli, D., Casalis, L., Parisse, P. 2022. Triple Negative Breast Cancer-derived Small Extracellular Vesicles as Modulator of Biomechanics in target cells. Nanomedicine 44, 102582, doi: 10.1016/j.nano.2022.102582.
78. Serra-Picamal, X., Conte, V., Vincent, R., Anon, E., Tambe, D.T., Bazellieres, E., Butler, J.P., Fredberg, J.J., Trepat, X. 2012. Mechanical waves during tissue expansion. Nature Phys. 8(8), 628-634, DOI: 10.1038/nphys2355.
79. Sosa, R.I., Galante, M., Tkatchenko, A. 2025. Power of the many-body force: magnitudes and angles of atomic van der Waals dispersion forces in extended molecular systems. Small Structures 6(10), e2500226, https://doi.org/10.1002/sstr.202500226.
80. Stirbat, T.V., Mgharbel, A., Bodennec, S., Ferri, K., Mertani, H.C., Rieu, J.P., Delanoe¨-Ayari, H. 2013. Fine Tuning of Tissues' Viscosity and Surface Tension through Contractility Suggests a New Role for a-Catenin. PLOS ONE 8(2), e52554, DOI: 10.1371/journal.pone.0052554.
81. Stringer, C., Wang, T., Michaelos, M., Pachitariu, M. 2021. Cellpose: A generalist algorithm for cellular segmentation. Nature Meth. 18(1), 100–106, https://doi.org/10.1038/s41592-020-01018-x.
82. Stroka, K.M., Jiang, H., Chen, S-H., Tong, Z., Wirtz, D., Sun, S.X., Konstantopoulos, K. 2014. Water permeation drives tumor cell migration in confined microenvironments. Cell, 157(3), 611–623, doi:10.1016/j.cell.2014.02.052.
83. Takayanagi, M., Uemura, S., Shunsuke, M. 1964. Application of Equivalent Model Method to Dynamic Rheo-Optical Properties of Crystalline Polymer. J Polym. Sci. Part C 5 113-122, doi.org/10.1002/polc.5070050111.
84. Tlili, S., Gauquelin, E., Li, B., Cardoso, O., Ladoux, B., Delanoë-Ayari, H., Graner, F. 2018. Collective cell migration without proliferation: density determines cell velocity and wave velocity. R. Soc. Open Sci. 5, 172421, https://doi.org/10.1098/rsos.172421.
85. Tkatchenko, A., DiStasio, R.A.Jr., Car, R., Scheffler, M. 2012. Accurate and efficient method for many-body van der Waals interactions. Phys. Rev. Lett. 108(23), 236402, https://doi.org/10.1103/PhysRevLett.108.236402.
86. Tse, J.M., Cheng, G., Tyrrell, J.A., Wilcox-Adelman, S.A., Boucher, Y., Jain, R.K., et al. 2012. Mechanical compression drives cancer cells toward invasive phenotype. PNAS 109(3), 911–49 DOI: 10.1073/pnas.1118910109.
87. Zhang, Y., Xu, G., Lee, R.M., Zhu, Z., Wu, J., Liao, S., Zhang, G., Sun, Y., Mogilner, A., Losert, W., et al. 2017. Collective cell migration has distinct directionality and speed dynamics. Cell Mol. Life Sci. 74:3841–3850, DOI: 10.1007/s00018-017-2553-6.

88. Zhao, J., Naveed, H., Kachalo, S., Cao, Y., Tian, W., Liang, J. 2013. Dynamic mechanical finite element model of biological cells for studying cellular pattern formation. 35th Annual International Conference of the IEEE EMBS Osaka, Japan, 3 - 7 July, 2013, 4517- 4520.